Title

The Impact of Fatty Acid and Aldehyde on Myoglobin Redox Chemistry

Author

Germolus, Clayton Bruce

Publication Date

2021

Peer reviewed|Thesis/dissertation

The Impact of Fatty Acid and Aldehyde on Myoglobin Redox Chemistry

By

CLAYTON BRUCE GERMOLUS

THESIS

Submitted in partial satisfaction of the requirements for the degree of

MASTER OF SCIENCE

in

Biophysics

in the

OFFICE OF GRADUATE STUDIES

of the

UNIVERSITY OF CALIFORNIA

DAVIS

Approved:

Thomas Jue, Chair

Robert Fairclough

Tsung-Yu Chen

Committee in Charge

2022

Abstract

Myoglobin (Mb) is a monomeric protein commonly thought to mediate facilitated diffusion of O_2 in muscle tissue and serve as a store for O_2. Provocative experiments have revealed reason to doubt this orthodox view of Mb function. In-vivo NMR experiments suggest the diffusion rate of Mb in the cell is too slow to significantly contribute to mitochondrial oxygen flux at physiological pO_2, cardiac performance and respiration are not impaired in perfused murine heart in the presence of CO, and the Mb pool in terrestrial mammals can only sustain respiration for a few seconds. Most intriguingly of all, experiments with Mb-knockout (MbKO) mice have measured a shift in metabolic substrate preference from fatty acids (FA) to glucose (Glc), but no deficits in exercise ability compared to wild-type mice. These findings have inspired further research into Mb function. Studies have observed that the lipid oxidation product, 4-hydroxy-2-nonenal (HNE), increases MbO_2 auto-oxidation, and several NMR studies have observed binding between Mb and several common fatty acids (FA).

The present study attempts to explore unanswered questions about the significance of these interactions by measuring the effect of HNE and common FA on Mb auto-oxidation and electron transfer (ET) between Mb and cytochrome C (Cyt C). No interactions between HNE and Mb were detected by NMR, and no significant enhancement of Mb auto-oxidation or electron transfer by HNE were measured. By contrast, there was a significant increase in Mb auto-oxidation in the presence of Oleic Acid, and a significant decrease in electron transfer to Cyt C in the presence of Lauric Acid. Palmitic Acid did not significantly alter either reaction rate. Though unanswered questions remain, Mb's centrality as a model for the relationship between protein structure and function presents a rationale for further study of Mb – FA interactions.

Dedication

To my parents, who have always encouraged me to learn as much as I can, to believe in myself, and as Robert Ingersoll once said: “to grasp the torch that they had held and hold it high, that light might conquer darkness still”.

Acknowledgement

First, I would like to offer my sincere gratitude to my adviser and mentor, Dr. Thomas Jue, for taking me under his wing and pouring his time and expertise into guiding my development as a young scientist. His passion for science for the sake of genuine intellectual curiosity, rather than simply chasing after the next grant, is all too rare in our current day. I would also like to thank Dr. Robert Fairclough and Dr. Tsung-Yu Chen for their wise counsel, and for volunteering their time as members of my thesis committee to ensure the quality of this finished work. Likewise, thank you to Dr. Jeffrey Walton and Dr. Ping Yu of the NMR facility, for all their assistance in learning NMR spectroscopy, and their exceptional patience when my experiments ran into difficulties.

I also offer my profound thanks to Dr. Eric Mann and Dr. Jonathan Bragg of the Microbiology Department for being fantastic mentors and for offering me the opportunity to help shape the intellectual development of hundreds of undergraduate students as a teaching assistant. To Brittany Greenwood and the rest of the MIC103L teaching assistants who I had the pleasure of working with, who were always willing to lend a helping hand whenever a student stumped me with a question.

To my graduate cohort: Dr. Jan Maly and Jessica Gregory—the Three Musketeers, through thick and thin. It was a rocky journey at times, but we've finally made it! To Dr. Amjad Ramahi, with whom I spent many a long night of diligent writing so we could finally, as Dr. Jue put it, just get the [expletive] thing done. To Usman Rehman, who is going to be an exceptional PhD scientist in the very near future if my experience collaborating with him is any indication.

To my beloved friends of Clan Barborc: Gary Cline, Dr. Brent Follin, Dr. Santona Tuli, Emily Quinn Finney, and Hannah Eilers. Your love and support during my darkest moments

enabled me to find the inner strength to keep climbing upward. I never would have made it across the finish line without all of you.

Last, but far from least, I would like to thank my family. My mother, Sharon, who's bottomless well of unconditional love probably violates the laws of thermodynamics, even if I can't prove it. My father, Bruce, who will forever be my role model and hooked me on science for life when he introduced me to *The Golden Treasury of Natural History*, by Bertha Morris Parker. My grandmother, Dixie, who bakes the world’s best pineapple pie. My brother, Nicholas, the Waluigi to my Wario—two oddballs forever seeking the finest of life's many treasures.

Table of Contents

Chapter I

Introduction

INTRODUCTION

Myoglobin (Mb) is a monomeric, predominantly alpha-helical protein with a molecular weight of approximately 17 kilodaltons (2). The helical domains encase a heme group consisting of a single iron atom coordinated to a porphyrin ring, **Figure 1-1A**. The heme's association with the larger peptide chain is stabilized by interactions with two histidine residues at positions 93 and 64, referred to as the proximal and distal histidines, respectively. The x-ray crystal structure of Mb was the first protein structure determined (16) and earned Dr. John Kendrew the 1962 Nobel Prize in Chemistry. It ushered in a revolution in structural biology. Thanks in large part to its well-characterized oxygen (O_2) binding activity, **Figure 1-1B**, Mb is still cited as a model for illustrating the relationship between protein structure and function in biochemistry courses. Its function is commonly thought to consist of mediating facilitated diffusion of O_2 in muscle tissue and O_2 storage (24, 25). In muscle, the measured concentrations have ranged from 0.1-0.4 mM (5).

A closer examination of the scientific literature reveals reason to doubt the orthodox view of Mb's function. If Mb were to serve as a vital oxygen store, one would expect it to sustain oxidative phosphorylation during hypoxia. Indeed, diving mammals, such as sperm whales, rely on their high Mb store during extended dives while hunting (6). However, the concentration of Mb in terrestrial mammals, far lower than in whales, can only sustain respiratory consumption for a few seconds (4). Indeed, even when CO blocks all Mb oxygen binding capacity, cardiac performance and respiration are not impaired in perfused murine heart, **Figure 1-2** (3, 11). Perhaps most intriguingly of all, experiments with Mb-knockout (MbKO) mice have failed to measure significant deficits in sustained exercise ability compared to wild-type mice, **Figure 1-**

3A (10, 12). Taken together, these findings suggest that Mb does not appear essential in maintaining normal muscle function.

Even though MbKO mice do not exhibit any physiological deficits, their metabolic substrate preference shifts from fatty acids (FA) to glucose (Glc). Relative to wild type myocardium, the MbKO mouse shifts its metabolism from 3/1 to 0.7/1 FA metabolism/glycolysis, **Figure 1-3B** (9). This has been attributed to a reduction in Mb-mediated O_2 transport (9), given the aerobic nature of fatty acid catabolism. This hypothesis seems plausible so long as Mb can act as an efficient oxygen transporter.

However, recent in-vivo NMR measurements suggest the diffusion rate of Mb in the cell is too slow to significantly contribute to mitochondrial oxygen flux at physiological O_2 pressure (pO_2) (17, 18). These results cast doubt on Mb's viability as a mediator of facilitated diffusion altogether. Since Mb cannot compete effectively with free O_2, how does maintaining near-millimolar concentrations of this inefficient oxygen transport protein benefit the cell? What then causes the increased preference for glucose over FA in MbKO murine heart, if Mb facilitated O_2 diffusion does not play a significant role? The answer may lie in an affinity between Mb and the FA themselves. Indeed, recent NMR studies suggest that Mb can interact with several common varieties of FA, **Figure 1-4** (14, 21-23). Intriguingly, titration with increasing quantities of PA reveals a selective perturbation of the heme pocket at the site of the 8-Me (13.2 ppm), **Figure 1-5**, suggesting the possibility of a specific binding site (22, 23).

The research described herein explores this hypothesized interaction between Mb and FA to characterize how FA binding to Mb can alter the protein's physiological function. ^{1}H NMR experiments have demonstrated that FA binding to Mb has a carbon chain length dependence (14). FA does not interact significantly with Mb at carbon chain lengths below 12. Moreover,

studies have shown that palmitate (PA), which has carbon chain length of 16, will bind selectively to Mb (14, 21-23), without altering its O_2 binding affinity (15).

Numerous experiments, however, have reported that a lipid oxidation product can increase the rate of metMb formation. Specifically, the addition of a 9 carbon 4-hydroxynon-2-enal (HNE), **Figure 1-6A,** resulted in a measurable increase in Mb auto-oxidation, **Figure 1-6B** (1, 7, 8, 13). This observation appears incongruent with previous NMR studies, which suggest saturated FA of carbon chain length at or below 10 do not bind Mb (14), while those of chain length 12 and above do. Whether the 9-carbon unsaturated HNE (nonenal) can interact with Mb poses a puzzling question.

Thus, the research in this thesis has first focused on the interaction of HNE with Mb to test the validity of the NMR interpretation and to determine if HNE interaction, if detected, can alter Mb auto-oxidation and electron transfer. It then subsequently examines if fatty acid interaction will alter Mb auto-oxidation and electron transfer.

Both spectrophotometric and NMR measurements find no evidence to support any HNE binding to Mb. In contrast to previous observations, the present study does not detect any HNE induced increase in Mb auto-oxidation or electron transfer to a protein acceptor, cytochrome C (26). However, lauric acid alters the rate of electron transfer, while oleic acid increases Mb auto-oxidation. The research in this thesis supports the NMR interpretation of a carbon chain length dependent FA interaction with Mb. It also indicates that FA has different effects on redox properties of Mb and its O_2 binding affinity. This research has then established an approach to clarify how FA alters Mb function in the cell.

Figure Captions

Figure 1-1

A) Structure of the Mb heme pocket, with His64 over the CO ligand, and His93 coordinated to the central iron atom (20).

B) O_2 saturation curve of human Mb at varying temperatures (19).

Figure 1-2

Bar graph displaying oxygen consumption rate (MVO_2), rate-pressure product (RPP), and phosphocreatine (PCr) concentration in murine myocardium at 540 beats/min, with and without CO. CO prevents Mb binding to O_2 but results in no significant change in any of the measured parameters. (3)

Figure 1-3

A) Graphic comparison of exercise performance in wild-type and MbKO mice. MbKO mice exhibit no significant deficits in exercise ability compared to wild-type mice (10).

B) Bar graph comparing metabolism of Glc and PA in wild-type and MbKO mice. MbKO mice exhibit a significant increase in Glc utilization at the expense of PA catabolism (9).

Figure 1-4

^{1}H-NMR spectra of 0.8 mM MbCN 8 heme methyl signal (13.2 ppm) in the presence of varying amounts of FA in 30 mM Tris and 3.2 mM TSP at pH 7.4 and 35 °C using the following FA:Mb ratios: 0:1, 0.2:1, 0.5:1, 1:1, 2:1, and 4:1. (A) Octanoic Acid (OCT), (B) Decanoic Acid (DEC), (C) Lauric Acid (LAU), (D) Myristic Acid (MYR), (E) Palmitic Acid (PAM). OCT does not induce any change. DEC shifts slightly upfield. PAM induces intensity loss and an upfield shift in Mb signal. Significant changes are measured in the presence of LAU and MYR (14).

Figure 1-5

^{1}H NMR spectra of 0.8 mM MbCN with and without palmitate in Tris buffer at pH 7.4 35 °C: (A) Control spectrum of 0.8 mM MbCN. (B) Spectrum of 0.8 mM MbCN with 0.8 mM TSP and with PA at a PA:Mb ratio of 0.4:1. (C) Difference spectrum (Spectra A–B). The peaks at 26.4, 17.9, and 13.2 ppm correspond to the 5, 1 and 8 heme methyl groups. Addition of PA results in a selective reduction in 8 heme methyl peak intensity (23).

Figure 1-6

A) Chemical structure of 4-hydroxynon-2-enal (HNE).

B) MetMb formation in auto-oxidation assays of MbO_2 and various saturated and unsaturated aldehydes during incubation at pH 7.4 and 37 °C. Addition of unsaturated aldehydes, all with carbon chain length <12, result in an increased auto-oxidation rate (7).

References

1. **Alderton AL, Faustman C, Liebler DC, and Hill DW**. Induction of redox instability of bovine myoglobin by adduction with 4-hydroxy-2-nonenal. *Biochemistry* 42: 4398-4405, 2003.
2. **Antonini E, and Brunori M**. *Hemoglobin and Myoglobin in their Reactions with Ligands*. Amsterdam: North-Holland Publishing Company, 1971.
3. **Chung Y, Huang SJ, Glabe A, and Jue T**. Implication of CO inactivation on myoglobin function. *Am J Physiol Cell Physiol* 290: C1616-1624, 2006.
4. **Chung Y, and Jue T**. Cellular response to reperfused oxygen in the postischemic myocardium. *American Journal of Physiology - Heart and Circulatory Physiology* 271: H687-H695, 1996.
5. **Chung Y, Mole PA, Sailasuta N, Tran TK, Hurd R, and Jue T**. Control of respiration and bioenergetics during muscle contraction. *AJP: Cell Physiology* 288: C730-C738, 2004.
6. **Dolar ML, Suarez P, Ponganis PJ, and Kooyman GL**. Myoglobin in pelagic small cetaceans. *Journal of Experimental Biology* 202: 227-236, 1999.
7. **Faustman C, Liebler DC, McClure TD, and Sun Q**. α,β-Unsaturated aldehydes accelerate oxymyoglobin oxidation. *Journal of Agricultural and Food Chemistry* 47: 3140-3144, 1999.
8. **Faustman C, Sun Q, Mancini R, and Suman SP**. Myoglobin and lipid oxidation interactions: mechanistic bases and control. *Meat Sci* 86: 86-94, 2010.
9. **Flögel U, and Laussmann T**. Lack of Myoglobin Causes a Switch in Cardiac Substrate Selection. *Circulation Research* 96: e68-e75, 2005.
10. **Garry DJ, Ordway GA, Lorenz JN, Radford NB, Chin ER, Grange RW, Bassel-Duby R, and Williams RS**. Mice without myoglobin. *Nature* 395: 905-908, 1998.
11. **Glabe A, Chung Y, Xu D, and Jue T**. Carbon monoxide inhibition of regulatory pathways in myocardium. *Am J Physiol* 274: H2143-2151, 1998.
12. **Godecke A, Flogel U, Zanger K, Ding Z, Hirchenhain J, Decking UKM, and Schrader J**. Disruption of myoglobin in mice induces multiple compensatory mechanisms. *Proceedings of the National Academy of Sciences* 96: 10495-10500, 1999.
13. **Grunwald EW, Tatiyaborworntham N, Faustman C, and Richards MP**. Effect of 4-hydroxy-2-nonenal on myoglobin-mediated lipid oxidation when varying histidine content and hemin affinity. *Food Chem* 227: 289-297, 2017.
14. **Jue T, Shih L, and Chung Y**. Differential Interaction of Myoglobin with Select Fatty Acids of Carbon Chain Lengths C8 to C16. *Lipids* 52: 711-727, 2017.
15. **Jue T, Simond G, Wright TJ, Shih L, Chung Y, Sriram R, Kreutzer U, and Davis RW**. Effect of fatty acid interaction on myoglobin oxygen affinity and triglyceride metabolism. *J Physiol Biochem* 2017.
16. **Kendrew JC, Bodo G, Dintzis HM, Parrish RG, Wyckoff H, and Phillips DC**. A Three-Dimensional Model of the Myoglobin Molecule Obtained by X-Ray Analysis. *Separation and isolation of fractions of rabbit gamma-globulin containing the antibody and antigenic combining sites* 182: 670-671, 1958.
17. **Lin PC, Kreutzer U, and Jue T**. Anisotropy and temperature dependence of myoglobin translational diffusion in myocardium: Implication for oxygen transport and cellular architecture. *Biophysical Journal* 92: 2608-2620, 2007.

18. **Lin PC, Kreutzer U, and Jue T**. Myoglobin translational diffusion in rat myocardium and its implication on intracellular oxygen transport. *Journal of Physiology* 578: 595-603, 2007.
19. **Rossi-Fanelli A, and Antonini E**. Studies on the oxygen and carbon monoxide equilibria of human myoglobin. *Archives of Biochemistry and Biophysics* 77: 478-492, 1958.
20. **Rovira C, Schulze B, Eichinger M, Evanseck JD, and Parrinello M**. Influence of the heme pocket conformation on the structure and vibrations of the Fe-CO bond in myoglobin: A QM/MM density functional study. *Biophysical Journal* 81: 435-445, 2001.
21. **Shih L, Chung Y, Sriram R, and Jue T**. Interaction of Myoglobin with Oleic Acid. *Chem Phys Lipids* 91: 165-171, 2015.
22. **Shih L, Chung Y, Sriram R, and Jue T**. Palmitate interaction with physiological states of myoglobin. *Biochimica et Biophysica Acta - General Subjects* 1840: 656-666, 2014.
23. **Sriram R, Kreutzer U, Shih L, and Jue T**. Interaction of fatty acid with myoglobin. *FEBS Letters* 582: 3643-3649, 2008.
24. **Wittenberg BA, and Wittenberg JB**. Transport of Oxygen in Muscle. *Annu Rev Physiol* 51: 857-878, 1989.
25. **Wittenberg JB**. Myoglobin-Facilitated Oxygen Diffusion: Role of Myoglobin in Oxygen Entry into Muscle. *Physiological reviews* 50: 559-636, 1970.
26. **Wu CS, Duffy P, and Brown WD**. Interaction of myoglobin and cytochrome C. *J Biol Chem* 247: 1899-1903, 1972.

Figure 1-1

A

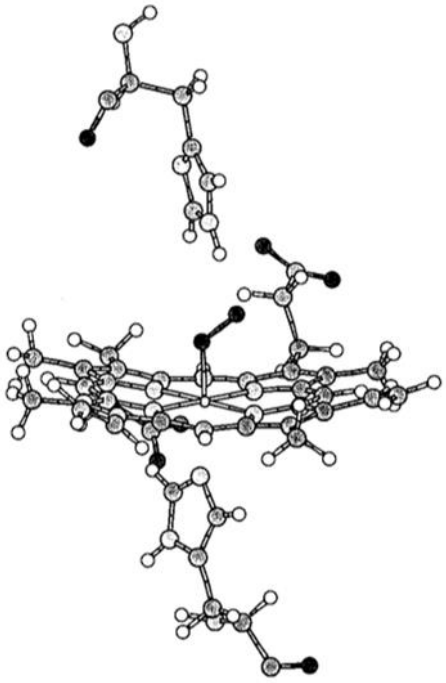

B

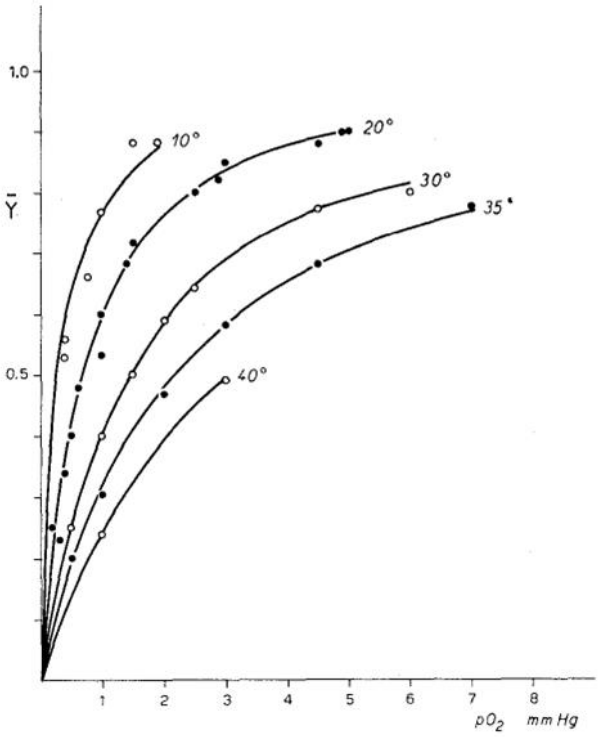

A) **Rovira C, et al.** *Biophysical Journal* 81: 435-445, 2001.

B) **Rossi-Fanelli A, and Antonini E**. *Archives of Biochemistry and Biophysics* 77: 478-492, 1958.

Figure 1-2

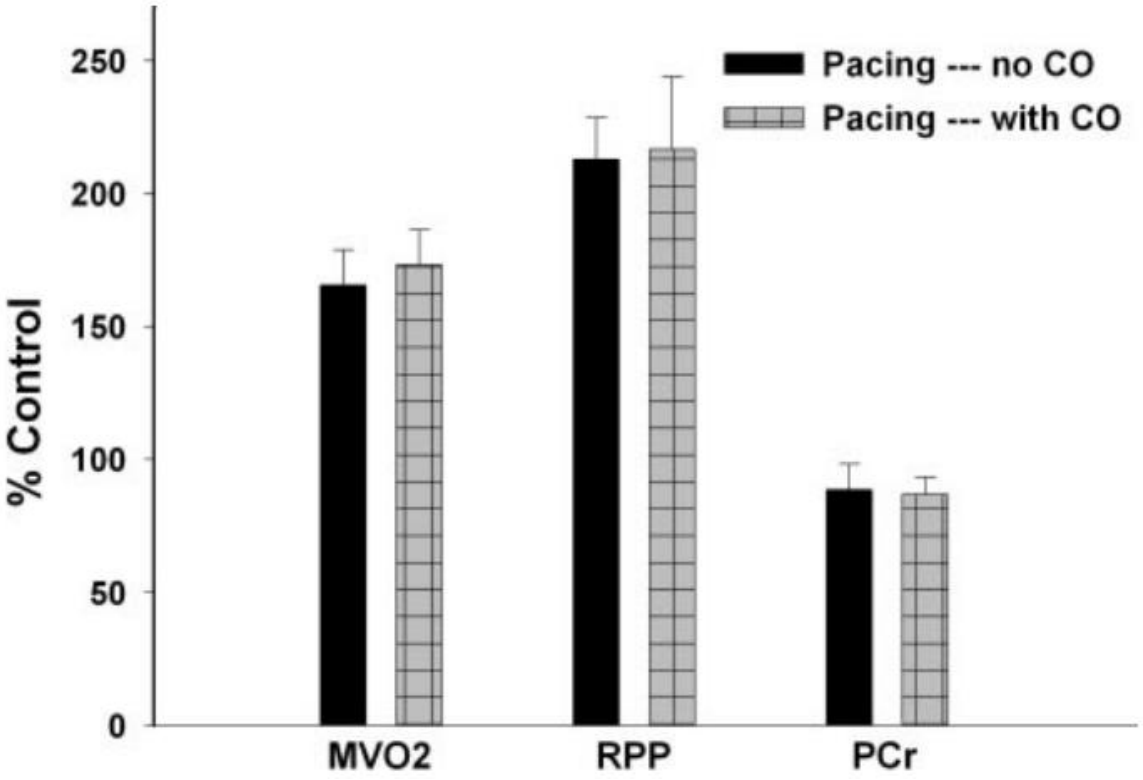

Chung Y, et al. *Am J Physiol Cell Physiol* 290: C1616-1624, 2006.

Figure 1-3

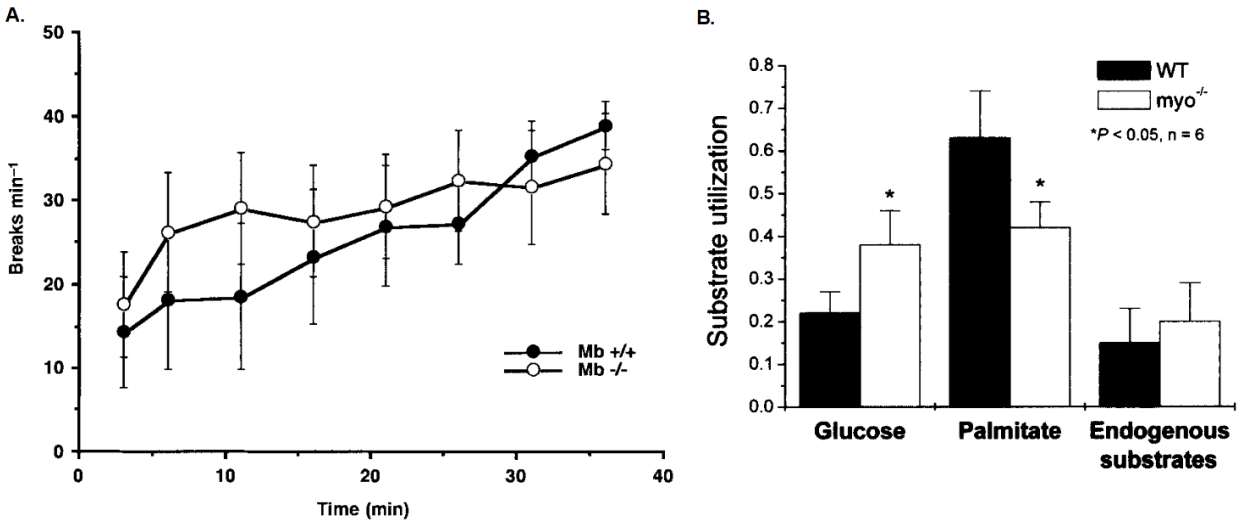

A) **Garry DJ, et al.** *Nature* 395: 905-908, 1998.

B) **Flögel U, et al.** *Circulation Research* 96: e68-e75, 2005.

Figure 1-4

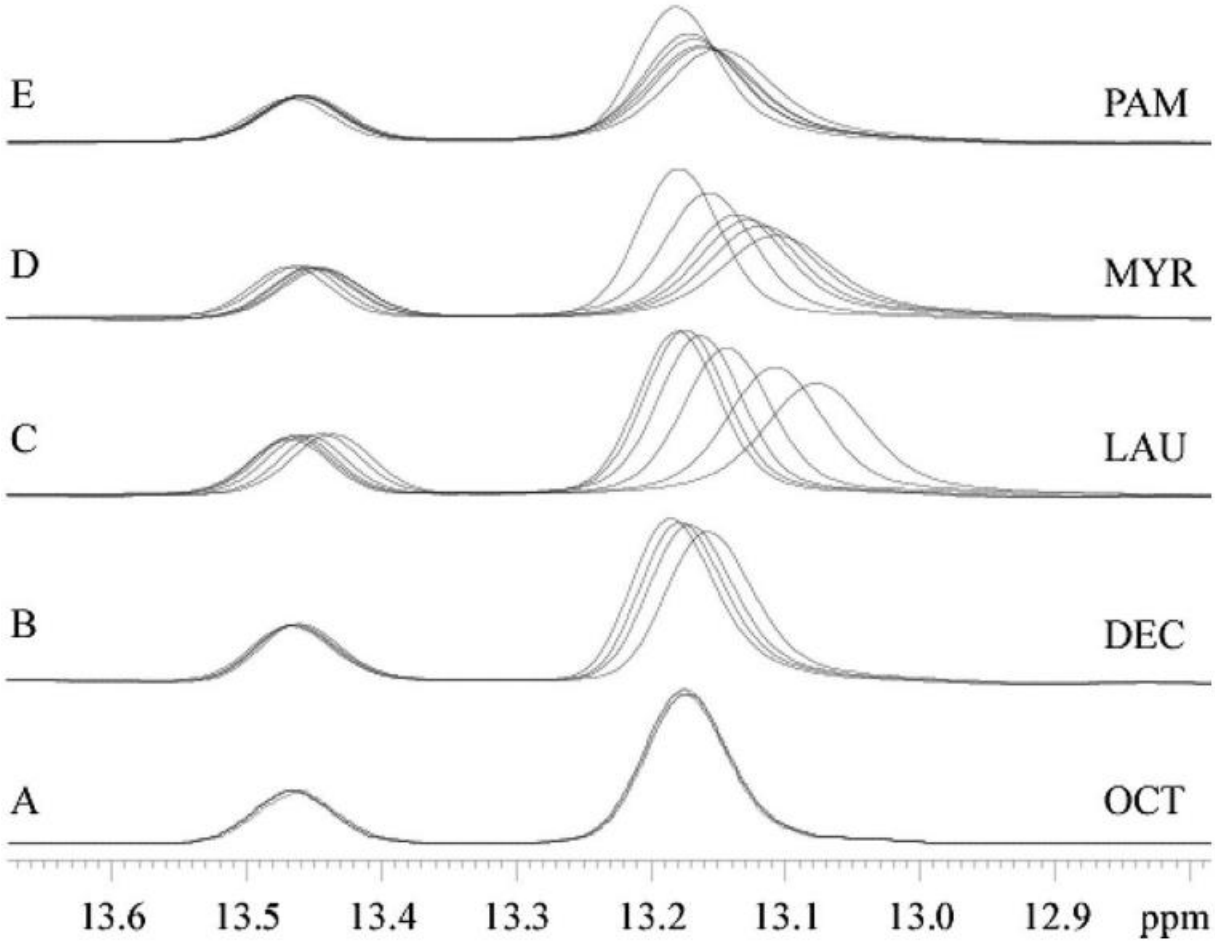

Adapted from **Jue T, et al**. *Lipids* 52: 711-727, 2017.

Figure 1-5

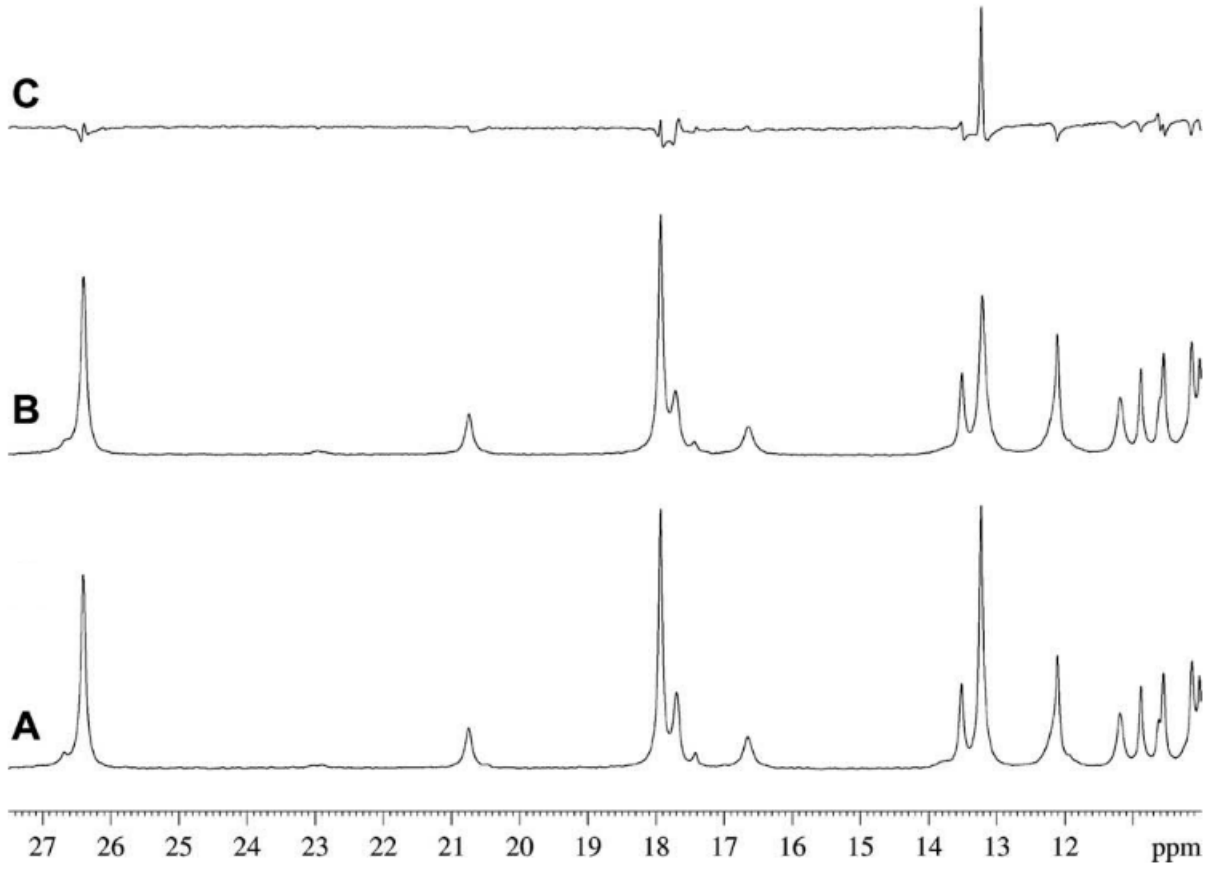

Adapted from **Sriram R, et al**. *FEBS Letters* 582: 3643-3649, 2008.

Figure 1-6

A

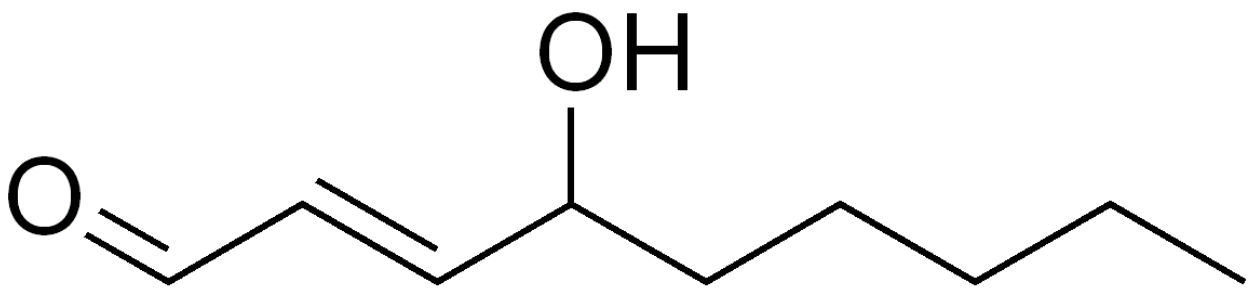

B

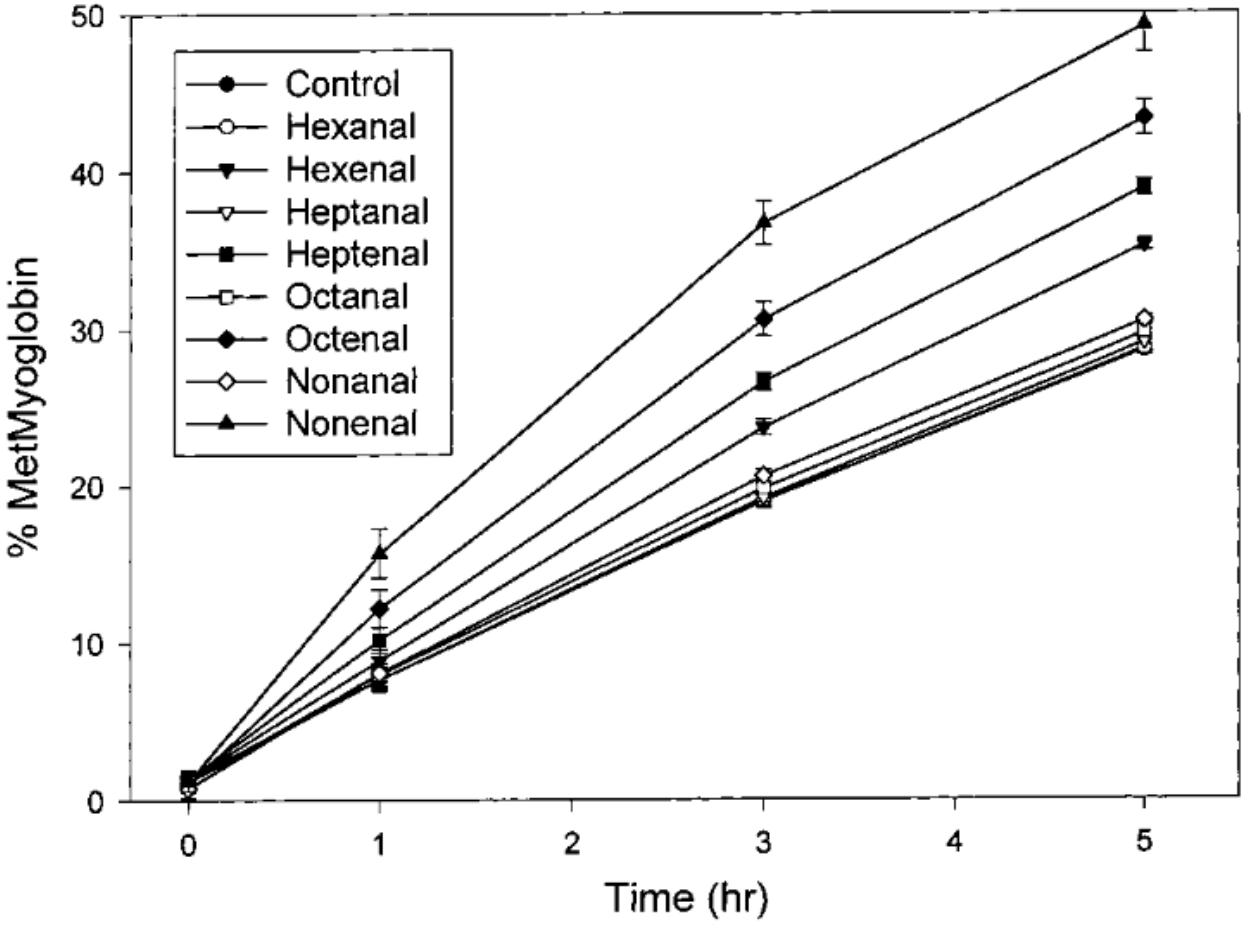

B**) Faustman C, et al**. *Journal of Agricultural and Food Chemistry* 47: 3140-3144, 1999.

Chapter II

Impact of Nonenal on Myoglobin Oxidation

Abstract

Provocative studies have observed that the lipid oxidation product, 4-hydroxy-2-nonenal (HNE), increases MbO_2 auto-oxidation, which in turn can potentially accelerate lipid oxidation. NMR studies have noted that fatty acids can bind to Mb and can compete effectively with fatty acid binding protein (FABP) to transport fatty acid in skeletal muscle. However, only fatty acids with carbon chain length greater than 10 interact with Mb. At and below a carbon chain length of 10, saturated fatty acids do not bind specifically or non-specifically to Mb. Whether the 9-carbon unsaturated HNE can interact with Mb poses then an unresolved question. The present study does not observe HNE interacting with Mb or enhancing Mb auto-oxidation or electron transfer. Nevertheless, the study has established an approach to clarify a central question in food chemistry: the role of Mb in lipid oxidation.

INTRODUCTION

Conventional biochemistry asserts that myoglobin (Mb) plays a central role as an O_2 store and as a facilitator of O_2 transport. Indeed, researchers have shown Mb supplying O_2 in plants, in mammals, and during seal apnea (17). Although *in vitro* studies support Mb's purported role in the cell, *in vivo* studies have found inconsistent evidence. At most, the total Mb store in terrestrial mammalian heart can sustain respiration for seconds during anoxia (8). Inhibiting Mb function with CO does not impair cardiac performance and respiration (7). Even a mouse without Mb exhibits no marked deficits in respiration, contractile function, and bioenergetics (15, 16). In fact, Mb *in situ* diffuses too slowly to compete effectively with free O_2 in the cell (24, 25). These puzzling observations raise fundamental questions about the function of Mb in the cell and have spurred research into a controversial role for Mb as an NO scavenger and as a reductase (12). Some studies do not support the envisioned Mb's role in regulating NO (21, 23). Despite the reassurances in the biochemistry and physiology canon, the cellular function of Mb remains uncertain (17, 37).

The struggle to understand Mb's role in regulating O_2 consumption often overlooks Mb's role in redox biology (3). In contrast, food scientists have well-recognized the importance of Mb's participation in multiple reactions that oxidize lipid. With lipid oxidation, food spoils and meat quality degrades (14). Even though Mb and lipid oxidation correlates, defining the mechanisms remains elusive. In part, the experiments must partition the contribution of multiple oxidation states of Mb (+2, MbO_2 and deoxy Mb; +3, metMb; and +4, perferryl and ferryl Mb). Each form of Mb has a reaction pathway in the initiation and progression of lipid oxidation. Even cross-linked Mb, hemochrome, hemichrome, hemin, and Fe can participate in lipid oxidation.

Nevertheless, experiments have observed that a lipid oxidation product increases metMb formation. Specifically, the common lipid oxidation product in food, 4-hydroxynon-2-enal (HNE), **Figure 2-1**, can increase Mb auto-oxidation (1, 11, 18). In forming metMb, MbO_2 can release a reactive superoxide, which then participates in the formation of H_2O_2. In the presence of H_2O_2, metMb can form the very reactive perferryl Mb and ferryl Mb. Consequently, HNE serves as part of a positive feedback loop to accelerate lipid oxidation. However, the HNE mechanism has validity, only if Mb interacts significantly with fatty acids.

Indeed, NMR has observed fatty acids binding specifically and non-specifically to Mb (31, 32). In fact, Mb can compete effectively with fatty acid binding protein (FABP) to transport fatty acid and obviate a complex mechanism to release fatty acids at the target site. Even though NMR studies show fatty acid binding to Mb, the interaction has a carbon chain length dependence. At and below a carbon chain length of 10, saturated fatty acids do not bind specifically or non-specifically to Mb (20). At and above a carbon chain length of 12, saturated fatty acids specifically and non-specifically bind to Mb. Whether the 9-carbon unsaturated HNE (nonenal) can interact with Mb poses an unresolved question.

The present study has examined the interaction of HNE with Mb and cannot find spectrophotometric or NMR evidence to support any binding to Mb. Nonenal also does not increase Mb auto-oxidation or Mb oxidation via electron transfer to a protein acceptor, cytochrome C (38). Even though nonenal does not appear to alter the Mb oxidation rate, other lipid oxidation products still can. The study establishes then an approach to investigate further the relationship between Mb and lipid oxidation, which will help clarify a central question in food chemistry.

METHODS

Protein Sample Preparation

Equine heart metmyoglobin (metMb) from Sigma Chemical and equine heart cytochrome c Type VI (Cyt C^{3+}) from Lee Biosolutions were dissolved in 30 mM Tris buffer (pH 7.4 with 1 mM EDTA) and used with no further processing. MbCO samples were prepared by introducing CO before reducing the metMb to MbCO with sodium dithionite ($Na_2S_2O_4$) (2, 32). A Sephadex G-25 column removed residual dithionite. Additional CO was added to produce the MbCO stock solution as confirmed spectrophotometrically by the appearance of the 540 and 579 nm peaks. MbO_2 was prepared by photolyzing the MbCO stock solution in the presence of the O_2 and light. The appearance of the 542 and 580 nm peaks confirmed the conversion of MbCO to MbO_2.

Equine heart ferricytochrome c (Cyt C^{3+}; Lee Biosolutions) was dissolved in 30 mM Tris/1 mM EDTA buffer pH 7.4. A ten-fold excess of potassium ferricyanide oxidized the residual Cyt C^{2+} to Cyt C^{3+}. A Sephadex G-25 column removed the ferricyanide. Complete oxidation of Cyt C^{2+} to Cyt C^{3+} was measured spectrophotometrically by the appearance of the Cyt C^{3+} peak at 530 nm and the disappearance of the Cyt C^{2+} peaks at 520 and 550 nm.

Ferrocytochrome (Cyt C^{2+}) was produced from sodium dithionite reduction of Cyt C^{3+} in 30 mM Tris/1 mM EDTA buffer pH 7.4. A Sephadex G-25 column removed any residual dithionite. Spectrophotometric assessment of Cyt C^{3+} signal at 530 nm and the Cyt C^{2+} peaks at 520 and 550 nm assayed the extent of the reduction reaction. The optical spectra show millimolar extinction coefficients for the peak maxima as follows: MbO_2, 580 nm, 14.4; Cyt C^{3+}. 530 nm, 10.1; metMb, 530 nm, 6.6; and Cyt C^{2+} 550 nm, 27.7. At 630 nm, metMb exhibits an extinction coefficient of 0.25 (2, 28)

HNE Sample Preparation

Samples of 4-hydroxy-2-nonenal (HNE) were prepared by injecting 15μL of stock 10 mg/mL 4-HNE solution (Cayman Chemical Company) into a microcentrifuge tube in ice. Passing N_2 gas over the sample evaporated the ethanol. The sample was then diluted with 30 mM Tris/1 mM EDTA buffer pH 7.4 to generate a solution of approximately 0.6 mM. UV spectrophotometric assay determined the HNE concentration with the absorbance at 224 nm. Titrating the appropriate amount of HNE into Mb solution produce the HNE:Mb mixture of 1:1 and 4:1. The stock HNE solution was used immediately or was stored at -80°C for subsequent use.

Optical Measurement of Auto-oxidation and Electron Transfer

A Thermo-Fisher Evolution Array spectrophotometer followed Mb auto-oxidation and electron transfer. MbO_2 was diluted with 30 mM Tris/1 mM EDTA buffer pH 7.4 to reach a final concentration of 50μM for the auto-oxidation experiments and 8μM for the electron transfer experiments. Stock HNE was diluted and added, if appropriate, to the Mb solution to produce the required HNE:Mb molar ratio of 1:1 or 4:1. For the Mb electron transfer experiments, Cyt C^{3+} was added to initiate the reaction at Cyt C:Mb ratio of 1:1. A multi-sample Peltier block connected to a heated water bath (Heated Immersion Circulator SC 100, Thermo Scientific) maintained the sample temperature at 35°C. For auto-oxidation experiments requiring the addition of ethanol, 15μL of 95% ethanol was added for every 1 mL of reaction mixture to reach a final concentration of 1.5%.

Both the auto-oxidation and electron transfer experiments lasted for 2 hours, and the spectrophotometer acquired a spectrum every 5 minutes. Each spectrum comprised of signals averaged over 100 scans. Each scan required 9s of signal averaging. In the auto-oxidation

experiments, the deconvoluted MbO_2 peaks at 542 and 580 and the metMb peak at 630 nm tracked the reaction kinetics. In the electron transfer experiments, the changes in the deconvoluted signals of MbO_2 at 580 nm, metMb at 630 nm, Cyt C^{3+} at 530 nm, and Cyt C^{2+} at 520 and 550 nm followed the reaction. Baseline corrections used the data values from 780-820 nm.

Deconvolution Algorithm

A deconvolution algorithm determined the respective MbO_2, metMb, Cyt C^{3+}, and Cyt C^{2+}contribution based on a comparative analysis of select absorbances from the reference and the observed spectra as specified by

$$S_R = A_{R\text{-}MbO2} + A_{R\text{-}metMb} + A_{R\text{-}Cyt\ C2+} + A_{R\text{-}Cyt\ C3+}$$

$$S_O = A_{O\text{-}MbO2} + A_{O\text{-}metMb} + A_{O\text{-}Cyt\ C2+} + A_{O\text{-}Cyt\ C3+}$$

where $A_{R\text{-}x}$ = set of reference absorbances from species x, and $A_{O\text{-}x}$ = observed absorbances from species y. S_R and So denote the overall reference and observed spectra, respectively.

Reference spectra were collected for each reactant/product component at 8μM and 50 μM. These spectra provided a basis to scale the reference absorbances to the match the observed absorbances. The analysis leads to the calculated concentrations for each chemical species at different time intervals during the reaction kinetics. Each reference spectrum was calibrated against reported reference extinction coefficients, which provided the basis to determine the extinction coefficients at all other wavelengths in the spectral dataset (2, 28). The algorithm uses

the initial concentration to set the initial absorbance values and the reaction stoichiometry to constrain the reactant-product ratios during the reaction kinetics.

Even though the Thermo-Fisher Evolution Array collected discrete signals with 1 nm resolution from 190 nm to 1100 nm, only the signals from 500 to 650 nm in 1 nm steps were used to constitute the reference spectra $A_{R\text{-}x}$. The analysis compared then observed absorbances $A_{O\text{-}x}$ with $A_{R\text{-}x}$:

$$A_{R\text{-}MbO2} = A_{R\text{-}MbO2\ 500} + A_{R\text{-}MbO2\ 501} + A_{R\text{-}MbO2\ 502} \ldots A_{R\text{-}MbO2\ 650}$$

$$A_{R\text{-}metMb} = A_{R\text{-}metMb\ 500} + A_{R\text{-}metMb\ 501} + A_{R\text{-}metMb\ 502} \ldots A_{R\text{-}metMb\ 650}$$

$$A_{R\text{-}Cyt\ C2+} = A_{R\text{-}CytC\ 2+500} + A_{R\text{-}\ CytC2+\ 501} + A_{R\text{-}\ CytC2+\ 502} \ldots A_{R\text{-}\ CytC2+\ 650}$$

$$A_{R\text{-}Cyt\ C3+} = A_{R\text{-}CytC3+\ 500} + A_{R\text{-}\ CytC3+\ 501} + A_{R\text{-}\ CytC3+\ 502} \ldots A_{R\text{-}\ CytC3+\ 650}$$

$$A_{O\text{-}MbO2} = A_{O\text{-}MbO2\ 500} + A_{O\text{-}MbO2\ 501} + A_{O\text{-}MbO2\ 502} \ldots A_{O\text{-}MbO2\ 650}$$

$$A_{O\text{-}metMb} = A_{O\text{-}metMb\ 500} + A_{O\text{-}metMb\ 501} + A_{O\text{-}metMb\ 502} \ldots A_{O\text{-}metMb\ 650}$$

$$A_{O\text{-}Cyt\ C2+} = A_{O\text{-}CytC2+\ 500} + A_{O\text{-}\ CytC2+\ 501} + A_{O\text{-}\ CytC2+\ 502} \ldots A_{O\text{-}\ CytC2+\ 650}$$

$$A_{O\text{-}Cyt\ C3+} = A_{O\text{-}CytC3+\ 500} + A_{O\text{-}\ CytC3+\ 501} + A_{O\text{-}\ CytC3+\ 502} \ldots A_{O\text{-}\ CytC3+\ 650}$$

A 2-component system characterized Mb auto-oxidation,

$$S_R = [A_{R\text{-}MbO2,}\ A_{R\text{-}metMb}]$$

$$S_O = [A_{O\text{-}MbO2}, A_{O\text{-}metMb}]$$

while a 4-component system characterized the Mb to Cyt C electron transfer.

$$S_R = [A_{R\text{-}MbO2}, A_{R\text{-}metMb}, A_{R\text{-}Cyt\ C2+}, A_{R\text{-}Cyt\ C3+}]$$

$$S_O = [A_{O\text{-}MbO2}, A_{O\text{-}metMb}, A_{O\text{-}Cyt\ C2+}, A_{O\text{-}Cyt\ C3+}]$$

Scaling S_R to match S_O by minimizing the error (ΔE) leads to the quantitative determination of S_O.

The analysis used the reaction stoichiometry to constrain the algorithm

$$MbO_2 + Cyt\ C^{3+} = metMb + Cyt\ C^{2+}$$

$$MbO_2 = metMb + O_2$$

and set as a constant the fractional amount of (MbO_2+metMb)/total Mb and (Cyt C^{3+}+ Cyt C^{2+})/total Cyt C = 1.

Based on the initial concentrations, the reaction stoichiometry, reference spectrum of each reactant and product, and the reference extinction coefficients, the algorithm adjusted the difference in the reference and observed spectra to minimize the error using the least squares

algorithm in Microsoft Excel Solver. The minimization routine used all signals from 500-650 nm at a 1 nm spectrophotometer resolution. Minimizing the error in matching S_R to S_O leads to quantitative determination of S_O and the associated observed concentration, C_O. For all experiments, the percent error in the 580 nm MbO_2 peak ($\frac{A_O - A_R}{A_O}$ x 100) ranges from 0.01-0.46%.

For the Mb auto-oxidation, the algorithm returned the fractional amount of MbO_2 and metMb at each time point. For Mb electron transfer to Cyt C, the algorithm returned the fractional amount of MbO_2, metMb, Cyt C^{3+} and Cyt C^{2+}at each time point. The analysis was repeated for data set from each time point of the kinetics experiment. The determined concentration of each reaction component provided then the values for the kinetics analysis. An upcoming manuscript will provide a detailed analysis of the deconvolution approach.

Kinetic Analysis

The kinetic analysis of MbO_2 auto-oxidation assumed a 1st order reaction,

$$\mathrm{dA/A} = -kdt$$

and the linearized equation in the form $\ln(A/A_0) = -kt$ time determined the first-order rate constant from the slope. The equation $t_{1/2} = \frac{\ln(2)}{k}$ determined the reaction half-life from the rate constant.

For the Mb electron transfer reaction, the analysis assumed a 2nd order reaction,

$$dA/A = -kA^2dt$$

A linearized plot of $\frac{1}{A} = \frac{1}{A_0} + kt$ yielded a graph where the slope reflected the second-order rate constant. The equation, $t_{1/2} = 1/kA_0$ determined the reaction half-life from the 2nd order rate constant.

NMR

A Bruker Avance 600 MHz spectrometer recorded the ^1H NMR signals using a 5 mm probe. The ^1H 90° pulse, calibrated against the HOD signal from a 0.15 M NaCl solution, was 7.5μs. A Watergate pulse sequence suppressed the water signal. Sodium-3-(trimethylsilyl)-2,2,3,3-tetradeuteropropionic acid (TSP) served as the internal chemical shift and concentration reference. All samples contained 10% D_2O for deuterium lock. All measurements were carried out at 35° C. A typical spectrum required 512 scans and used the following signal acquisition parameters: 60 kHz spectral width, 8k data points, and 100ms recycle time. Signal processing applied an exponential window function before analysis.

Data Processing and Analysis

Data was expressed as mean value ± standard deviation (STDEV). Statistical and graphing analysis used both SigmaPlot (Systat Software, Inc., Point Richmond, CA) and Microsoft Excel. Significance was determined by Student's t-test and the single-factor analysis of variance (ANOVA) using an alpha (α) value of 0.05.

RESULTS

Figure 2-2 shows the reference visible spectra of 8 µM MbO_2, metMb, Cyt C^{3+}, and Cyt C^{2+} in 30 mM Tris/1 mM EDTA buffer pH 7.40 at 35°C. MbO_2 maxima appear at 542 and 580 nm; Cyt C^{3+} at 530 nm; Cyt C^{2+} at 550 nm. MetMb exhibits a clear signal at 630 nm. The spectral deconvolution algorithm uses the signals from 500 nm to 650 nm at 1 nm resolution to scale the 4-component reference spectra to best fit the observed spectra. The algorithm minimizes the error and leads to the determination of all reactant and product concentrations. The MbO_2 peak at 580 nm exhibits a percent error ($\frac{A_O - A_R}{A_O}$ x 100) ranging from 0.01-0.46%.

During auto-oxidation, the prominent MbO_2 peaks at 542 and 580 nm decrease, while the metMb peak at 630 nm increases, **Figure 2-3**. **Figure 2-3A** shows select spectra collected without HNE, while **Figure 2-3B** displays the select spectra collected in the presence of HNE. **Figure 2-3C** shows select spectra for the MbO_2 electron transfer without HNE, while **Figure 2-3D** shows the select spectra for electron transfer with HNE. During electron transfer from MbO_2 to Cyt C^{3+}, the MbO_2 peaks at 542 and 580 nm decrease along with Cyt C^{3+} peak at 530 nm. In contrast, Cyt C^{2+} peaks at 520 and 550 nm and the metMb peak at 630 nm increase.

Figure 2-4A plots $\ln([MbO_2]/[MbO_2]_0)$ vs time and shows the initial MbO_2 auto-oxidation kinetics with no HNE, with HNE, with HNE and 1.5% ethanol, and with only 1.5% ethanol. The linear regression of kinetics data yields the following equations: with no HNE: $Y=-1.64\times10^{-3}X$ ($R^2=1.00$), with HNE: $Y=-1.63\times10^{-3}X$ ($R^2=1.00$), with HNE and 1.5% ethanol: $Y=-2.05\times10^{-3}X$ ($R^2=1.00$), and with 1.5% ethanol: $Y=-2.00\times10^{-3}X$ ($R^2=0.99$). The slopes lead to the determination of the MbO_2 auto-oxidation rate constants.

Figure 2-4B plots 1/[MbO_2] vs time for the MbO_2 electron transfer reaction to Cyt C^{3+} with no HNE, with HNE, with HNE and 1.5% ethanol, and with 1.5% ethanol. The linear regression of the kinetics data yields the following equations: with no HNE: $Y=666X+12.5x10^4$ ($R^2=1.00$), with HNE: $Y=657X+12.5x10^4$ ($R^2=1.00$), with HNE and 1.5% ethanol: $Y=770X+12.5x10^4$ ($R^2=1.00$), and with 1.5% ethanol: $Y=764X+12.5x10^4$ ($R^2=1.00$)**.** The slope leads to determination of the rate constant for the electron transfer from MbO_2 to Cyt C[3]. Table 1 tabulates the MbO_2 auto-oxidation and electron transfer Cyt C rate constants.

A histogram of the MbO_2 auto-oxidation rate constants in the presence of HNE and ethanol+HNE shows the impact of HNE and ethanol, **Figure 2-5A**. Just the addition of HNE produces no significant difference in the Mb auto-oxidation rate ($F_{2,6}=0.30$, $P=0.75$). Similarly, the auto-oxidation rates in the presence of ethanol or ethanol + HNE do not differ significantly ($F_{2,6}=0.23$, $P=0.80$). However, using a single factor ANOVA to analyze the entire set of auto-oxidation rates indicates the presence of a significant factor, ethanol ($F_{5,12}=22.31$, $P < 0.01$).

The histogram of the rate constants for the MbO_2 to Cyt C^{3+} electron transfer reaction in the presence of HNE and ethanol + HNE displays the impact of HNE and ethanol, **Figure 2-5B**. Adding just HNE produces no significant difference in the electron transfer rate ($F_{2,6}=0.43$, $P=0.67$). Similarly, the electron transfer rate does not change significantly in the presence of ethanol or ethanol+HNE ($F_{2,6}=0.10$, $P=0.90$). Using a single factor ANOVA to analyze the entire set electron transfer reactions, however, indicates the presence of a significant factor, ethanol ($F_{5,12}=8.36$, $P < 0.01$).

Figure 2-6A shows the ^1H NMR spectra of MbCN in the presence of HNE. The hyperfine shifted 5-CH_3 (27 ppm), 1-CH_3 (18 ppm), and 8-CH_3 (13 ppm) heme signals show no perturbation upon the addition of HNE. Similarly, the diamagnetic region between 2-0 ppm also

detects no perturbation of the HNE signal. The difference spectrum shows the HNE signals in Mb solution matches the HNE signals observed in solution, **Figure 2-6B**.

However, the addition of HNE in the presence of 1.5% EtOH or in the addition of only 1.5% EtOH does alter the chemical shift position of the heme 8-CH_3 (13 ppm) and 1-CH_3 (18 ppm) signals. The heme 5-CH_3 (27 ppm) signal shows a smaller perturbation, **Figure 2-6C**.

DISCUSSION

Deconvolution Algorithm

In food science, optical measurements of the Mb and HNE interaction have routinely leaned on the Kryzwicki method (1, 9, 10, 22). The method assigns Mb signals at 545, 565, and 572 nm to represent deoxy Mb (DMb), MbO_2, and metMb. These peaks do not correspond to signal maxima. Using the Kryzwicki method has unfortunately led to negative values and checksum error in total Mb, which a modified Kryzwicki method has attempted to correct by using isosbestic points, absorbance maxima, and peaks with reduced signal overlap and interference. The modified Kryzwicki method assigns the signals at 503, 557, and 582 nm corresponding to metMb, DMb, and MbO_2 (34). However, the metMb signal at 503 nm still overlaps with a wing of the intense MbO_2 signal peaking at 542 nm. Even though the metMb signal has a 2:1 larger extinction coefficient than the MbO_2 signal at 503 nm, its signal still represents a very small fraction of the composite metMb/MbO_2 signal, and the dynamic interference from the MbO_2 peak at the beginning of an auto-oxidation experiment can still distort measurements of the initial kinetics. Such a potential dynamic interference at early time points of a kinetics measurement poses a challenge in the subsequent deconvolution and analysis.

The data from the initial time points can significantly alter the kinetics parameter determination. Oftentimes, studies have selected the 630 nm peak of metMb instead of the 503 nm peak, because it appears in a clear spectral window with a minimal interference from the MbO_2 spectra. Even though the 630 nm peak has a much lower extinction coefficient than the 503 nm peak, the MbO_2 peak interferes less.

The present study has ignored any DMb contribution, because given the 1.5 Torr partial pressure of oxygen required to saturate 50% of Mb (P50), no significant amount of DMb should exist in the reaction mixture during routine experiments under standard temperature and atmospheric pressure condition. A set of linear equations can characterize the reactants and products, and the analysis can solve these equations to determine the relative contributions under ideal conditions. Under experimental conditions, such an approach does not work effectively. Absorbances at different wavelengths overlap and require a judicious selection of wavelengths to avoid quantitation error arising from overlapping signals, which can have large dynamic range differences. However, choosing the spectral regions does not overcome baseline drift and other spectrophotometer errors that tend to plague the analysis of reactant and product concentration at the beginning and end of any reaction. In kinetics analysis, the initial points comprise a crucial set of data to determine the reaction rate. Using only MbO_2, metMb, Cyt C^{3+}, and Cyt C^{2+} signals from 500 nm to 650 nm has led to a fit of the observed and reference spectra with an error range between 0.10-0.46%.

HNE and Mb Auto-Oxidation

The literature has reported Mb auto-oxidation rates ranging from $0.9\text{-}2.2\text{x}10^{-3}$ min^{-1}, which depends upon the species, temperature, and pH. For equine Mb, the present study's analysis has determined an auto-oxidation rate constant of $1.64\text{x}10^{-3}$ min^{-1}. In the presence of

HNE at HNE:Mb ratios of 1:1 and 4:1, Mb auto-oxidation shows no significant change, $1.63x10^{-3}$ and $1.66x10^{-3}$ min^{-1}, respectively. Because previous studies added HNE in 1.5% ethanol to Mb, experiments tested the impact of ethanol. Indeed, adding HNE in a solution containing 1.5% ethanol increases significantly the MbO_2 auto-oxidation at HNE:Mb ratios 1:1 and 4:1 to $2.05x10^{-3}$ and $2.04x10^{-3}$ min^{-1}, respectively (10). However, in the presence of only 1.5% ethanol, Mb auto-oxidation also increases to $2.00x10^{-3}$ min^{-1}. The results implicate ethanol as the causative molecule increasing Mb auto-oxidation. HNE appears to have no effect.

^1H NMR results support the interpretation that nonenal does not bind to Mb. Previous studies have detected fatty acid interaction with Mb as reflected in changes in the heme signals of MbCN. Because of the paramagnetic interaction, select heme signals (27-13 ppm) shifted outside the typical diamagnetic spectral window between 0-10 ppm can reflect the fatty acid-Mb interaction. According to these NMR experiments, fatty acids interact with Mb, only if the fatty acid carbon chain length exceeds 10. Fatty acids with carbon chain lengths 10 or less do not interact with Mb. Fatty acids with carbon chain lengths 12-18, however, do interact with Mb and perturb the MbCN signals. Nonenal, at a carbon chain length of 9, does not produce any spectral perturbation. Even at an HNE:Mb ratio of 4:1, the MbCN spectra show no perturbation.

Difference spectra in the diamagnetic spectral region also does not detect any nonenal interaction with Mb. In the presence of Mb, the nonenal spectra match the one observed in buffer solution. The observations agree with the previous observations. Fatty acids with carbon chain lengths from 8 to 10 show no interaction with Mb, as evidenced by the unchanging chemical shift of the fatty acid $-CH_2$ peaks in the diamagnetic spectral region and the heme $-CH_3$ peaks. In contrast, fatty acids with carbon chain lengths of 12 or above show a marked shift in the fatty

acid-CH_2 peaks and the heme -CH_3 peaks. With nonenal, NMR detects no sign of any Mb interaction.

However, adding HNE in 1.5% ethanol or 1.5% ethanol perturbs the MbCN signal, especially the 8-heme methyl signal at 13.4 ppm. The shift in the 8-heme methyl reflects a change in electron-nuclear interaction resulting from a protein structural change induced by ethanol. HNE alone does not perturb the protein structure. The experimental observations point to ethanol as the source of a protein structural change and as a factor increasing auto-oxidation.

HNE and Mb Oxidation by Electron Transfer

Based on the standard reduction potentials of Mb (+0.046) and Cyt^{3+} C (+0.250) volts, Mb favors the transfer an electron to Cyt^{3+}C by 3392/1 (30, 35) . Spectrophotometry experiments have observed qualitatively the electron transfer from MbO_2 to Cyt^{3+} C, and researchers usually ascribe a superoxide anion release as the mechanism, because the rates of auto-oxidation and Cyt^{3+} C reduction appear to match (36, 38). However, experiments with modified ruthenium attached to histidine show that Mb can transfer readily the heme iron electron to the periphery without any superoxide radical formation (29).

The present study observes Mb transferring an electron to Cyt^{3+} C 2.3 times faster than Mb auto-oxidation. Moreover, deoxy Mb transfers an electron to Cyt^{3+} C, even though it cannot auto-oxidize to Fe^{3+} and does not form a superoxide radical (unpublished observation). Such observation suggests that Fe(II) Mb can transfer an electron independent of superoxide formation.

HNE also does not affect Mb oxidation by altering the electron transfer to an acceptor independent of superoxide formation. Control MbO_2 transfers an electron to Cyt^{3+} C with a 2nd

order rate constant of 666±23 M^{-1} min^{-1}. In the presence of HNE:Mb ratio of 1:1, the rate constant does not deviate, 657±32 M^{-1} min^{-1}. Even with HNE:Mb ratio of 4:1, the reaction does not change significantly, 676±22 M^{-1} min^{-1}. However, HNE:Mb ratios of 1:1 and 4:1 in the presence of 1.5% ethanol does change the electron transfer rate to Cyt^{3+} C to 770±57 and 780±35 M^{-1} min^{-1}, respectively. Just adding 1.5% ethanol to the Mb will change the rate of electron transfer to 764±28 M^{-1} min^{-1}. As in the case of auto-oxidation, HNE does not affect the electron transfer rate from MbO_2 to Cyt^{3+} C. Ethanol does. In contrast, MbO_2 in the presence of laurate or oleate will alter the rate of electron transfer from MbO_2 to Cyt^{3+} C as well as auto-oxidation (unpublished observation).

CONCLUSION

The role of Mb in the initiation and progression of lipid oxidation remains controversial and central to food chemistry. Many proposed mechanisms have focused on the critical step converting MbO_2 to metMb, because the reaction releases a reactive superoxide radical. The superoxide radical through dismutation can form H_2O_2, which in turn can convert Mb to the reactive perferryl Mb and ferryl Mb. These hypervalent Fe (IV) Mb exhibits pronounced pro-oxidative activity and can readily participate in lipid oxidation, which leads to food degradation. Because MbO_2 appears to have an electron transfer path independent of superoxide formation, Mb can participate in lipid oxidation via another reaction pathway. Even though HNE does not alter Mb auto-oxidation or electron transfer to Cyt C^{3+}, other fatty acids or lipid oxidation products may. From that vantage, the role of Mb in regulating cellular redox awaits additional experiments to clarify. The methodological approach described in the present paper can capture unique perspective on the complex Mb role in regulating lipid oxidation in food.

Figure Captions

Figure 2-1

Chemical structure of 4-hydroxynon-2-enal (HNE).

Figure 2-2

Reference spectra of 8 μM MbO_2, MetMb, Cyt C^{3+}, and Cyt C^{2+} at 35°C in 30 mM Tris/1 mM EDTA buffer pH 7.40 at 35°C. MbO_2 maxima appear at 542 and 580 nm; MetMb, 630 nm; Cyt C^{3+}, 530 nm; Cyt C^{2+}, 520 and 550 nm.

Figure 2-3

Select spectra of the MbO_2 auto-oxidation and electron transfer to Cyt C^{3+} of 8 or 50 μM MbO_2 in 30 mM Tris and 1 mM EDTA at pH 7.40 and 35°C. In auto-oxidation experiments, the MbO_2 peaks at 542 and 580 nm decrease, while the metMb peak at 630 nm increases. A) with no HNE and B) with HNE in HNE:Mb ratio of 1:1. In electrons transfer experiment, MbO_2 peaks at 542 and 580 nm decrease and Cyt C^{3+} peak at 530 nm decreases. Meanwhile, the Cyt C^{2+} peaks at 520 and 550 nm and the metMb peak at 630 nm increase C) with no HNE and D) with HNE in HNE:Mb ratio of 1:1. The spectrophotometer acquired a spectrum every 5 min over the 120 min time course.

Figure 2-4

Plot of MbO_2 vs time for auto-oxidation and electron transfer. A) For auto-oxidation of MbO_2 with no HNE, with 1:1 MbO_2:HNE, with 1:1 MbO_2:HNE + 1.5% ethanol (EtOH), and with only 1.5% EtOH, the plots of $\ln([MbO_2]/[MbO_2]_0)$ vs. time lead to the following linear regressions: without HNE: $Y=-1.64x10^{-3}X$ ($R^2=1.00$), with HNE: $Y=-1.63x10^{-3}X$ ($R^2=0.999$), with HNE and 1.5% EtOH: $Y=-2.05x10^{-3}X$ ($R^2=0.998$), with 1.5% EtOH: $Y=-2.00x10^{-3}X$ ($R^2=0.994$). B) For electron transfer from MbO_2 to Cyt C^{3+}, the plots of $1/[MbO_2]$ vs time at Mb:Cyt C ratio = 1 lead to following linear regressions: without HNE: $Y=0.067X+12.5x10^4$ ($R^2=0.999$), with HNE at HNE:MbO_2 ratio of 1: $Y=0.066X+12.5x10^4$ ($R^2=0.999$), with HNE and 1.5% EtOH: $Y=0.077X+12.5x10^4$ ($R^2=0.999$), and with 1.5% EtOH: $Y=0.076X+12.5x10^4$ ($R^2=0.999$).

Figure 2-5

Histograms of MbO_2 auto-oxidation and electron transfer rate constants at HNE:Mb ratios of 1:1 and 4:1 and in the presence or absence of EtOH. A) For MbO_2 auto-oxidation, only a single factor ANOVA of all 6 data sets indicates the presence of a significant factor, ethanol ($F_{5,12}=22.3$, $P < 0.01$). B) For electron transfer reaction, a single factor ANOVA of all 6 data sets also indicates the presence of a significant factor, ethanol ($F_{5,12} = 8.36$, $P < 0.01$).

Figure 2-6

^1H NMR spectra of 0.4 mM MbCN with and without 0.4 mM HNE in 30 mM Tris and 1 mM EDTA at pH 7.40 and at 35°C. A) Left panel: Spectra (30–10 ppm) of MbCN with no HNE, with

HNE, and difference spectra (bottom to top). The hyperfine shifted signals in the region show no interaction with HNE, as reflected in the prominent 5-CH_3 (26.9 ppm), 1-CH_3 (18.3 ppm), and 8-CH_3 (13.4 ppm) signals. B) Right panel: Spectra (2.0-0.2 ppm) of MbCN with no HNE, with HNE at HNE:Mb 4:1 ratio, difference spectrum with vertical scaling increased by 4 times, and solution spectra of 1.6 mM HNE (bottom to top). C) Spectra (30–10 ppm) of MbCN with no EtOH and with 1.5% EtOH. Top spectrum shows the difference (bottom to top). The heme 8-CH_3 (13.4 ppm) and 1-CH_3 (18.3 ppm) signals shift upfield with the addition of EtOH.

Table 2-1

MbO_2 Autoxidation and Electron Transfer to Cyt^{3+} C

	MbO_2 Autoxidation		**MbO_2 + Cyt^{3+} C**		**Sample**	**Condition**	**Reference**
MbO_2	**K min^{-1} x10^{-3}**	**$t_{1/2}$ min**	**K M^{-1} min^{-1}**	**$t_{1/2}$ min**			
CRL	-	-	801**	42**	s. whale	50mM, Pi, pH 7.5, 25°C	(38)
CRL	0.9±0.1	770±85	-	-	s. whale	0.1M Pi, 1 mM EDTA, pH 7, 37°C	(4)
CRL	2.17	320	-	-	s. whale	0.1M Pi, pH7, 30°C	(26)
CRL	1.6±0.2	433±54	-	-	bovine	0.1 M Pi, 31°C	(13)
CRL	1.32	526	-	-	bovine	10 mM Pi, 5 μM DTPA, 0.1 μM catalase, pH 6.0, 30°C	(19)
CRL	1.98	349	-	-	bovine	0.2 M Pi, pH 5.9, 37°C	(5)
CRL	1.33	520	-	-	bovine	0.4 M Pi/0.2 M citrate, pH 5.78, 22°C	(6)
CRL	1.64±0.04	423±9	666±23	188±6	equine	30 mM Tris/1 mM EDTA, pH 7.4, 35°C	This Work
CRL	1.33**	520**	-	-	equine	0.1 M Pi buffer, pH 7.2, 37°C	(27)
CRL	2.00±0.12	347±20	-	-	equine	50 mM Pi buffer, pH 7.2,	(33)

						37°C	
+1 HNE	1.63±0.05	426±14	657±32	191±9	equine		This Work
+4 HNE	1.66±0.04	418±10	676±22	185±6	equine		This Work
+EtOH	2.00±0.07*	348±13*	764±28	164±6	equine		This Work
+1 HNE +EtOH	2.05±0.09*	339±14*	770±57	163±12	equine		This Work
+4 HNE +EtOH	2.04±0.13*	341±22*	780±35	161±7	equine	0.1 M Pi, pH 7.2, 37°C	This Work
+6 HNE +EtOH	3.78	183	-	-	equine		(27)

*****ANOVA of the MbO_2 autoxidation reaction indicates ethanol as a significant factor ($F_{5,12}$=22.3, P=0.00001), and ANOVA of the MbO_2 and Cyt C^{3+} reaction indicates ethanol as a significant factor ($F_{5,12}$=8.36, P=0.001).

** Rate constants estimated from plotted kinetics.

s. whale = sperm whale.

References

1. **Alderton AL, Faustman C, Liebler DC, and Hill DW**. Induction of redox instability of bovine myoglobin by adduction with 4-hydroxy-2-nonenal. *Biochemistry* 42: 4398-4405, 2003.
2. **Antonini E, and Brunori M**. *Hemoglobin and Myoglobin in Their Reactions with Ligands*. Amsterdam: Elsevier/North Holland, 1971.
3. **Baron CP, and Andersen HJ**. Myoglobin-induced lipid oxidation. A review. *J Agric Food Chem* 50: 3887-3897, 2002.
4. **Brantley RE, Jr., Smerdon SJ, Wilkinson AJ, Singleton EW, and Olson JS**. The mechanism of autooxidation of myoglobin. *J Biol Chem* 268: 6995-7010, 1993.
5. **Brown WD, and Dolev A**. Autoxidation of Beef and Tuna Oxymyoglobins. *Journal of Food Science* 28: 207-&, 1963.
6. **Brown WD, and Mebine LB**. Autoxidation of Oxymyoglobins. *Journal of Biological Chemistry* 244: 6696-&, 1969.
7. **Chung Y, Huang SJ, Glabe A, and Jue T**. Implication of CO inactivation on myoglobin function. *Am J Physiol Cell Physiol* 290: C1616-1624, 2006.
8. **Chung Y, and Jue T**. Cellular response to reperfused oxygen in the postischemic myocardium. *Am J Physiol* 271: H687-H695, 1996.
9. **Faustman C, Liebler DC, and McClure TD**. Oxidation of myoglobin enhanced by adduction of 4-hydroxynonenal. *Faseb Journal* 12: A555-A555, 1998.
10. **Faustman C, Liebler DC, McClure TD, and Sun Q**. a,b unsaturated aldehydes accelerate oxymyoglobin oxidation. *Journal of Agricultural and Food Chemistry* 47: 3140-3144, 1999.
11. **Faustman C, Sun Q, Mancini R, and Suman SP**. Myoglobin and lipid oxidation interactions: mechanistic bases and control. *Meat Sci* 86: 86-94, 2010.
12. **Flogel U, Merx MW, Godecke A, Decking UKM, and Schrader J**. Myoglobin: A scavenger of bioactive NO. *ProcNatlAcadSci* 98: 735-740, 2001.
13. **Foucat L, Renerre M, Gatellier P, and Anton M**. 1H NMR Study of Bovine Myoglobin Autoxidation - Influence of Muscle-Type and Time Postmortem. *International Journal of Food Science and Technology* 29: 1-8, 1994.
14. **Frankel EN**. Lipid oxidation. *Prog Lipid Res* 19: 1-22, 1980.
15. **Garry DJ, Ordway GA, Lorenz JN, Radford NB, Chin ER, Grange RW, Bassel-Duby R, and Williams RS**. Mice without myoglobin. *Nature* 395: 905-908, 1998.
16. **Godecke A, Flogel U, Zanger K, Ding Z, Hirchenhain J, Decking UK, and Schrader J**. Disruption of myoglobin in mice induces multiple compensatory mechanisms. *ProcNatlAcadSciUSA* 96: 10495-10500, 1999.
17. **Gros G, Wittenberg B, and Jue T**. Myoglobin's old and new clothes: from molecular structure to function in living cells. *Journal of Experimental Biology* 213: 2713-2725, 2010.
18. **Grunwald EW, Tatiyaborworntham N, Faustman C, and Richards MP**. Effect of 4-hydroxy-2-nonenal on myoglobin-mediated lipid oxidation when varying histidine content and hemin affinity. *Food Chem* 227: 289-297, 2017.
19. **Gutzke D, and Trout GR**. Temperature and pH dependence of the autoxidation rate of bovine, ovine, porcine, and cervine oxymyoglobin isolated from three different muscles--Longissimus dorsi, Gluteus medius, and Biceps femoris. *J Agric Food Chem* 50: 2673-2678, 2002.

20. **Jue T, Shih L, and Chung Y**. Differential Interaction of Myoglobin with Select Fatty Acids of Carbon Chain Lengths C8 to C16. *Lipids* 52: 711-727, 2017.
21. **Kreutzer U, and Jue T**. Investigation of bioactive NO-scavenging role of myoglobin in myocardium. *Eur J Physiol* 452: 36-42, 2006.
22. **Krzywicki K**. The determination of haem pigments in meat. *Meat Sci* 7: 29-36, 1982.
23. **Li W, Jue T, Edwards J, Wang Z, and Hintze T**. Changes in Nitric Oxide Bioavailability Regulate Cardiac Oxygen Consumption:Control by Intramitochodrial SOD2 and Intracellular Myoglobin. *AJP - Heart and Circulatory Physiology* 286: H47-H54, 2004.
24. **Lin PC, Kreutzer U, and Jue T**. Anisotropy and temperature dependence of myoglobin translational diffusion in myocardium: implication for oxygen transport and cellular architecture. *Biophys J* 92: 2608-2620, 2007.
25. **Lin PC, Kreutzer U, and Jue T**. Myoglobin translational diffusion in rat myocardium and its implication on intracellular oxygen transport. *J Physiol* 578: 595-603, 2007.
26. **Livingston DJ, Watts DA, and Brown WD**. Myoglobin interspecies structural differences: effects on autoxidation and oxygenation. *Arch Biochem Biophys* 249: 106-115, 1986.
27. **Lynch MP, and Faustman C**. Effect of aldehyde lipid oxidation products on myoglobin. *Journal of Agricultural and Food Chemistry* 48: 600-604, 2000.
28. **Margoliash E, and Frohwirt N**. Spectrum of horse-heart cytochrome c. *Biochem J* 71: 570-572, 1959.
29. **Onuchic JN, Beratan DN, Winkler JR, and Gray HB**. Pathway analysis of protein electron-transfer reactions. *Annu Rev Biophys Biomol Struct* 21: 349-377, 1992.
30. **Rodkey FL, and Ball EG**. Oxidation-reduction potentials of cytochrome c. *Fed Proc* 6: 286, 1947.
31. **Shih L, Chung Y, Sriram R, and Jue T**. Interaction of myoglobin with oleic acid. *Chem Phys Lipids* 191: 115-122, 2015.
32. **Shih L, Chung Y, Sriram R, and Jue T**. Palmitate interaction with physiological states of myoglobin. *Biochim Biophys Acta* 1840: 656-666, 2014.
33. **Stewart JM**. Free fatty acids enhance the oxidation of oxymyoglobin and inhibit the peroxidase activity of metmyoglobin. *Biochem Cell Biol* 68: 1096-1102, 1990.
34. **Tang J, Faustman C, and Hoagland TA**. Krzywicki revisited: Equations for spectrophotometric determination of myoglobin redox forms in aqueous meat extracts. *Journal of Food Science* 69: C717-C720, 2004.
35. **Taylor JF, and Morgan VE**. Oxidation-reduction Potentials of the Metmyoglobin-myoglobin system. *J Biol Chem* 144: 15-20, 1942.
36. **Wallace WJ, Houtchens RA, Maxwell JC, and Caughey WS**. Mechanism of autooxidation for hemoglobins and myoglobins. Promotion of superoxide production by protons and anions. *J Biol Chem* 257: 4966-4977, 1982.
37. **Wittenberg JB, and Wittenberg BA**. Myoglobin function reassessed. *J ExpBiol* 206: 2011-2020, 2003.
38. **Wu CS, Duffy P, and Brown WD**. Interaction of myoglobin and cytochrome C. *J Biol Chem* 247: 1899-1903, 1972.

Figure 2-1

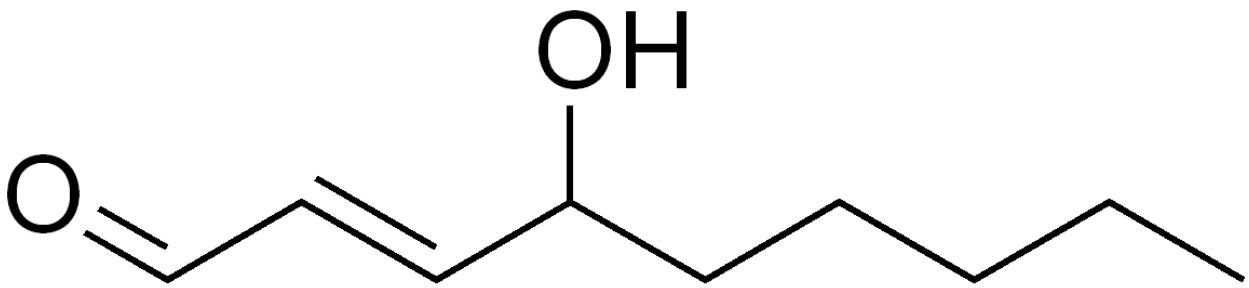

Figure 2-2

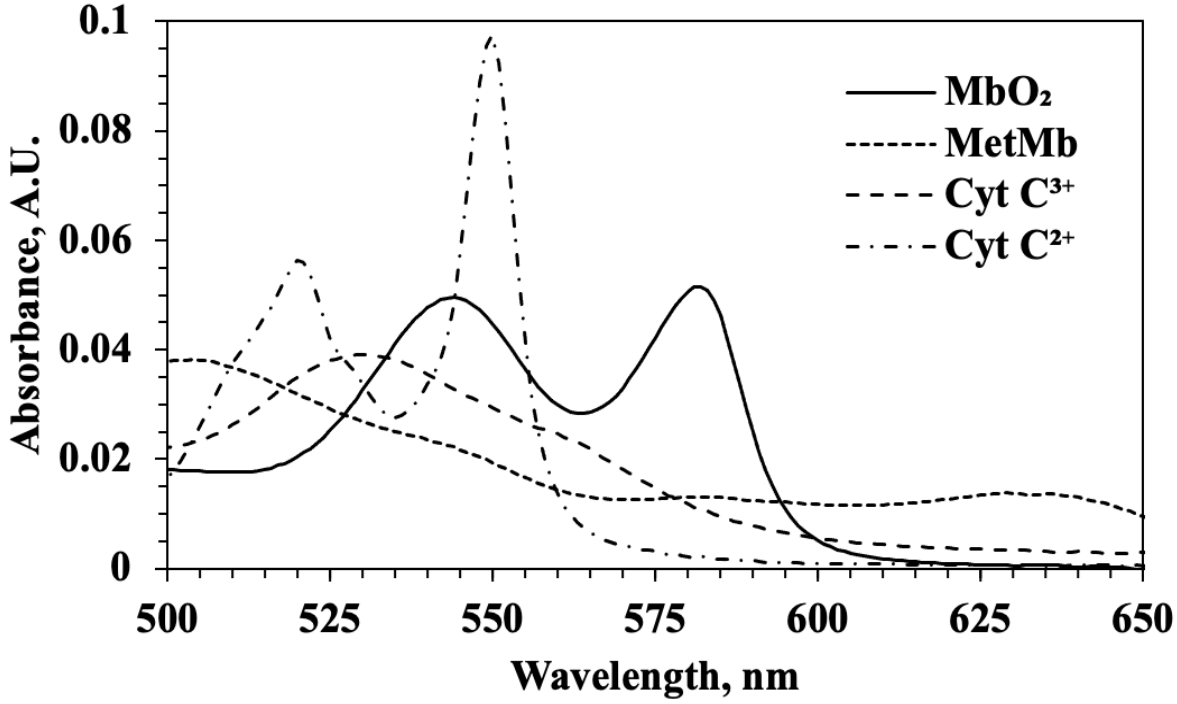
0.1
0.08
0.06
0.04
0.02
0
Absorbance, A.U.
500
525
550
575
600
625
650
Wavelength, nm
MbO₂
MetMb
Cyt C³⁺
Cyt C²⁺

Figure 2-3

A

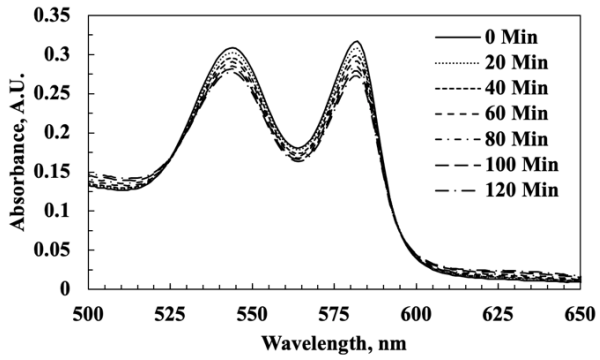

B

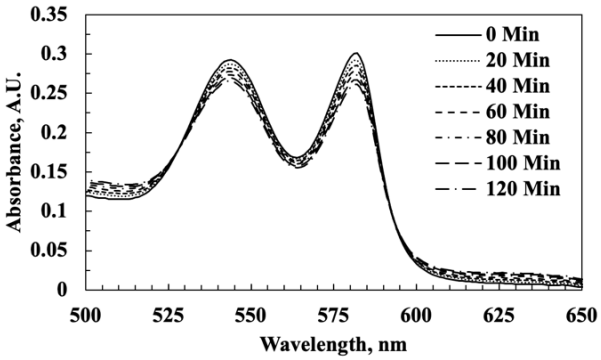

C

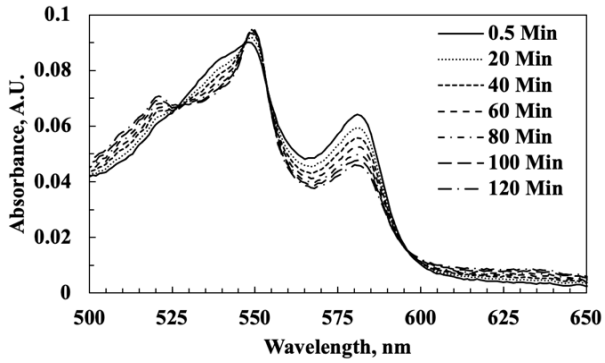

D

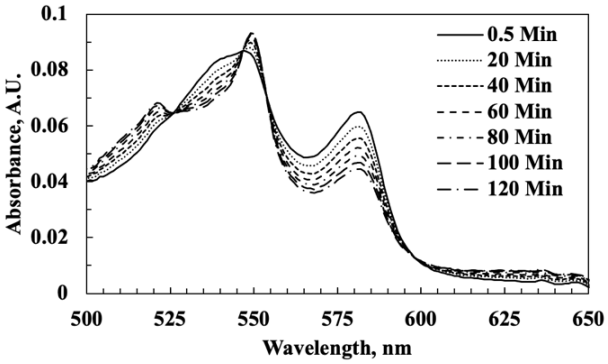

Figure 2-4

A

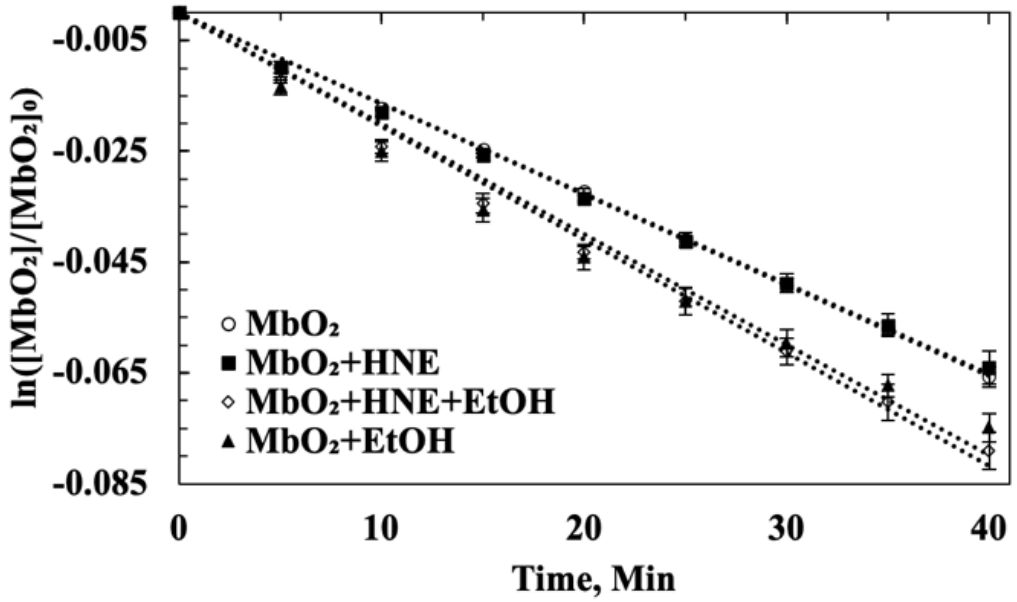
-0.005
-0.025
-0.045
-0.065
-0.085
ln([MbO₂]/[MbO₂]₀)
0
10
20
30
40
Time, Min
MbO₂
MbO₂+HNE
MbO₂+HNE+EtOH
MbO₂+EtOH

B

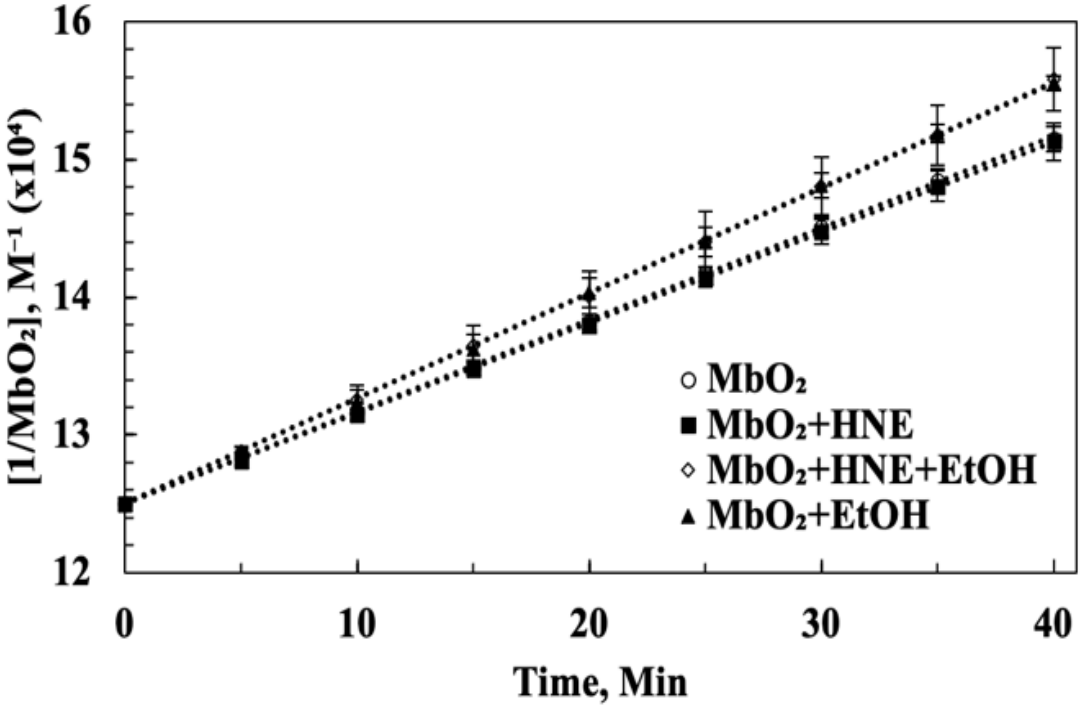
16
15
14
13
12
[1/MbO₂], M⁻¹ (x10⁴)
0
10
20
30
40
Time, Min
MbO₂
MbO₂+HNE
MbO₂+HNE+EtOH
MbO₂+EtOH

Figure 2-5

A

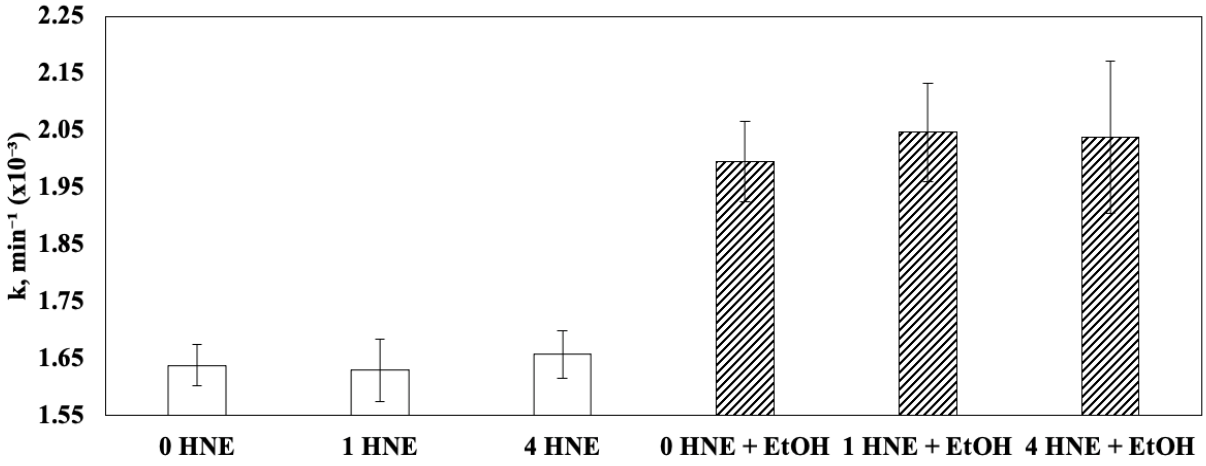
2.25
2.15
2.05
1.95
1.85
1.75
1.65
1.55
k, min⁻¹ (x10⁻³)
0 HNE
1 HNE
4 HNE
0 HNE + EtOH
1 HNE + EtOH
4 HNE + EtOH

B

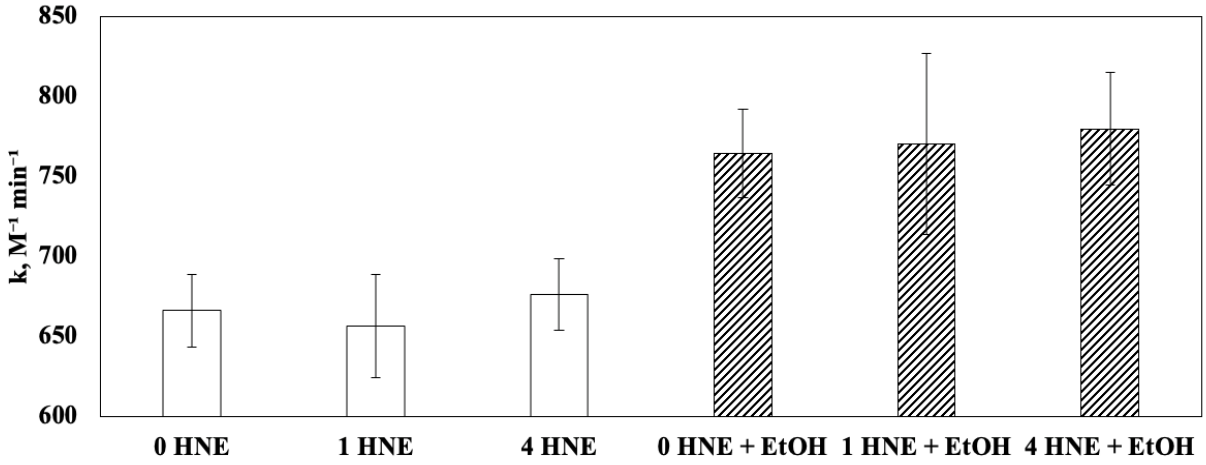
850
800
750
700
650
600
k, M⁻¹ min⁻¹
0 HNE
1 HNE
4 HNE
0 HNE + EtOH
1 HNE + EtOH
4 HNE + EtOH

Figure 2-6

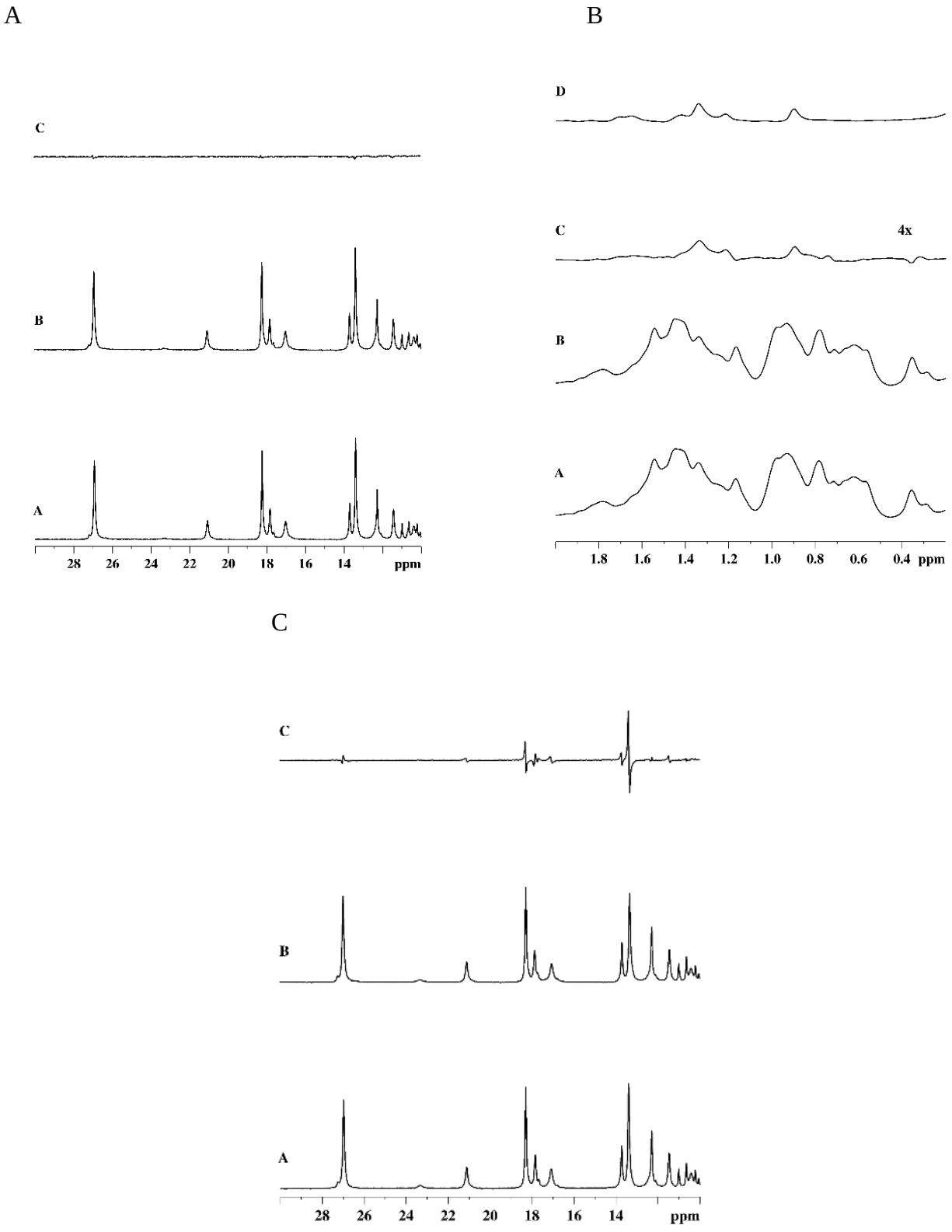
A
C
B
A
28 26 24 22 20 18 16 14 ppm
B
D
C
4x
B
A
1.8 1.6 1.4 1.2 1.0 0.8 0.6 0.4 ppm
C
C
B
A
28 26 24 22 20 18 16 14 ppm

Chapter III

The Impact of Fatty Acids on Myoglobin – Cytochrome C Redox

Abstract

Recent NMR studies have observed binding between myoglobin (Mb) and several common fatty acids (FA) of carbon chain length greater than 10. Questions about the significance of these interactions remain unresolved, with some studies indicating that Mb can compete effectively with fatty acid binding protein (FABP) as a means of intracellular FA transport. The present study expands on previous reports of an electron transfer (ET) reaction between Mb and cytochrome C (Cyt C) by characterizing the impact of FA binding on Mb redox chemistry. The present study observes a significant increase in Mb auto-oxidation in the presence of Oleic Acid, and a significant decrease in electron transfer to Cyt C in the presence of Lauric Acid. Palmitic Acid did not significantly alter either reaction rate. These findings and myoglobin's centrality as a model for the relationship between protein structure and function presents a rationale for further study of Mb – FA interactions.

INTRODUCTION

Myoglobin (Mb) is one of the most well-studied models of the protein structure – function relationship. It is commonly thought to mediate facilitated diffusion of O_2 in muscle tissue and serve as a cellular store for O_2 (17, 18). Recently, this view of Mb function has been challenged by in-vivo experiments revealing no significant loss cardiac performance in perfused rat myocardium when O_2 binding by Mb is inhibited by CO (3, 5). Perhaps more surprisingly, experiments with MbKO mice have not found significant deficits in exercise ability compared to wild type mice but have measured a relative increase in carbohydrate consumption at the expense of fatty acids (4, 6). Indeed, an accumulating body of data suggests a possible role for Mb in fatty acid (FA) metabolism, ranging from evidence of binding affinity with a variety of common FA(7, 15), to evidence of Mb being able to compete favorably with FA binding proteins (FABP) as a means of FA transport (8, 13, 14).

Additionally, Mb's redox chemistry remains fertile ground for study (2). Prior experiments have reported evidence of an electron transfer reaction between Mb and cytochrome c (Cyt C), in which ferrous Mb (Mb^{2+}) reduces ferricytochrome c (Cyt C^{3+}) (19). Calculation of an equilibrium constant using the Nernst equation and the standard reduction potentials of Mb (+0.046V) and Cyt C^{3+} (+0.250V) predicts such a reaction should favor product formation by a ratio of 3392/1 (12, 16), suggesting Cyt C is a viable redox partner for Mb.

The present study has sought to expand upon both observations by further characterizing the Mb – Cyt C electron transport reaction, differentiating it from Mb auto-oxidation and probing for the impact of FA interaction on both processes. In so doing, it has found evidence of acceleration of Mb auto-oxidation by oleic acid (OA) as well as significant slowing of the much

faster ET reaction by lauric acid (LA), while finding no evidence of significant modulation of either reaction by palmitic acid (PA). These findings raise further questions about the role of Mb in fatty acid metabolism, suggesting a possibly complex relationship between FA interaction and Mb redox chemistry.

METHODS

Sample Preparation

Metmyoglobin (metMb; Sigma Chemical Inc) from equine heart was dissolved in 30 mM Tris buffer (pH 7.4 with 1 mM EDTA) and used with no further processing. MbO_2 samples were prepared by purging dissolved O_2 with N_2 before reducing the metMb to Mb (II) with sodium dithionite ($Na_2S_2O_4$) (1, 11). A Sephadex G-25 column then removed residual dithionite. The procedure to prepare the Cyt C (II) sample followed the preparation procedure for MbO_2. Complete reduction of Cyt C (III) to Cyt C (II) was verified by measuring the appearance of the Cyt C (II) peak at 550nm.

Equine heart ferricytochrome c Type VI (Cyt C^{3+}; Lee Biosolutions) was dissolved in 30 mM Tris/1 mM EDTA buffer pH 7.4. A ten-fold excess of potassium ferricyanide oxidized the residual Cyt C^{2+} to Cyt C^{3+}. Ferricyanide was removed with a Sephadex G-25 column. Complete oxidation of Cyt C^{2+} to Cyt C^{3+} was measured spectrophotometrically by the appearance of the Cyt C^{3+} peak at 530 nm and the disappearance of the Cyt C^{2+} peaks at 520 and 550 nm.

Ferrocytochrome (Cyt C^{2+}) was produced via sodium dithionite reduction of Cyt C^{3+} in 30 mM Tris/1mM EDTA buffer pH 7.4. A Sephadex G-25 column removed any residual dithionite.

Complete reduction of Cyt C was confirmed via spectrophotometric measurement of Cyt C^{3+} signal at 530 nm and the Cyt C^{2+} peaks at 520 and 550 nm. The optical spectra show millimolar extinction coefficients for the following peaks: MbO_2, 580 nm, 14.4; Cyt C^{3+}. 530 nm, 10.1; metMb, 530 nm, 6.6; and Cyt C^{2+} 550 nm, 27.7. At 630 nm, metMb exhibits an extinction coefficient of 0.25 (1).

Palmitic, Oleic, and Lauric Acids were dissolved in 30 mM Tris, 1 mM EDTA, pH 8.5 buffer at 65° C. The resulting 5 mM fatty acid (FA) solutions were kept at 65° C using a Thermolyne 17600 Dri-Bath heating block prior to loading into cuvettes containing freshly prepared Mb samples. As the FA solution was only 1% of the total cuvette volume, their elevated temperature was assumed to have no significant effect on the overall reaction temperature.

Optical Spectroscopy

UV-Vis kinetic assays were conducted using a Thermo-Fisher Evolution Array spectrophotometer. Freshly prepared MbO_2 samples were loaded into cuvettes and diluted to a final concentration of 0.05 mM using pH 7.4 Tris buffer. During electron transfer experiments, an equimolar volume of Cyt C (III) was loaded immediately to initiate the reaction. Samples were held at 35° C using a multisample Peltier block connected to an MGW Lauda MT temperature regulated water bath.

Auto-oxidation and electron transfer experiments both lasted 2 hours, with the spectrophotometer acquiring a spectrum every 5 minutes. Each spectrum comprised of signals averaged over 100 scans. Each scan required 9s of signal averaging. Both experiment types followed the absorbance change in the Mb (II) β-band at 580nm to monitor the reaction kinetics (1). Baseline corrections used the data values from 780-820 nm.

Concentration Determination

The total absorbance of a mixture can be expressed as the sum of its component absorbances. For MbO_2,- Cyt C^{3+} electron transfer, this can be written as,

$$A_{app} = A_{MbO2} + A_{metMb} + A_{Cyt\ C\ 3} + A_{Cyt\ C2}$$

The change in apparent, or composite, absorbance (dA_{app}) can be expressed as,

$$dA_{app} = dA_{MbO2} + dA_{metMb} + dA_{Cyt\ C\ 3} + dA_{Cyt\ C\ 2}$$

Per the Beer-Lambert Law, each component absorbance can be written as,

$$A = \varepsilon\, \ell\, c$$

Yielding,

$$dA_{app} = \varepsilon_{MbO2}\ell\, dc_{MbO2} + \varepsilon_{metMb}\ell\, dc_{metMb} + \varepsilon_{Cyt\ C\ 3}\ell\, dc_{Cyt\ C\ 3} - \varepsilon_{Cyt\ \ C\ 2}\ell\, dc_{Cyt\ C\ 2}$$

The stoichiometry of MbO_2 – Cyt C^{3+} electron transfer is equimolar, so the rate of Mb oxidation must equal the rate of Cyt C reduction,

$$dc_{MbO2} = dc_{Cyt\ C\ 3}$$

$$dc_{metMb} = dc_{Cyt\ C\ 2}$$

$$dc_{MbO2} = - dc_{metMb}$$

$$dc_{Cyt\ C\ 3} = - dc_{Cyt\ C\ 2}$$

Yielding,

$$dAapp = \varepsilon_{MbO2}\, \ell\, dc_{MbO2} - \varepsilon_{metMb}\, \ell\, dc_{MbO2} + \varepsilon_{Cyt\ C\ 3}\, \ell\, dc_{MbO2} - \varepsilon_{Cyt\ C\ 2}\, \ell\, dc_{MbO2}$$

Which can be rewritten as,

$$dA_{app} = \ell\, dc_{MbO2}\, (\varepsilon_{MbO2} - \varepsilon_{metMb} + \varepsilon_{Cyt\ C\ 3} - \varepsilon_{Cyt\ C\ 2})$$

Yielding the following two equations,

$$dc_{MbO2} = dA_{app}/\ell(\varepsilon_{MbO2} - \varepsilon_{metMb} + \varepsilon_{Cyt\ C\ 3} - \varepsilon_{Cyt\ C\ 2})$$

$$dc_{MbO2} = dA_{app}/\ell(\varepsilon_{MbO2} - \varepsilon_{metMb})$$

MbO_2 concentrations at each time point were calculated using the change in absorbance at 580nm (A_{580}).

Kinetic Analysis

Kinetic analysis of MbO_2 auto-oxidation assumed a 1st order reaction,

$$\mathrm{dA/A} = -kdt$$

and the linearized equation in the form,

$$\ln\left(A/A_0\right) = -kt$$

determined the first-order rate constant from the slope. The equation $\mathrm{t}_{1/2} = \frac{\ln(2)}{k}$ determined the reaction half-life from the rate constant.

For the Mb electron transfer reaction, a 2nd order reaction was assumed,

$$\mathrm{dA/A} = -kA^2dt$$

A linearized plot of $\frac{1}{A} = \frac{1}{A_0} + kt$ yielded a graph where the slope reflected the second-order rate constant. The equation, $\mathrm{t}_{1/2} = 1/\mathrm{k}A_0$ determined the reaction half-life from the 2nd order rate constant.

Data Processing and Analysis

Data was expressed as mean value ± standard error (SE). SigmaPlot (Systat Software, Inc., Point Richmond, CA) and Microsoft Excel were used for analytic calculations. Significance was determined by Student's t-test using a p value of 0.05.

RESULTS

Figure 3-1A shows the reference visible spectra of 8 µM MbO_2, metMb, Cyt C^{3+}, and Cyt C^{2+} in 30 mM Tris/1 mM EDTA buffer pH 7.4 at 35°C. MbO_2 maxima appear at 542 and 580 nm; Cyt C^{3+} at 530 nm; Cyt C^{2+} at 550 nm. MetMb exhibits a clear signal at 630 nm. If the electron transfer reaction were to occur as predicted, one would therefore expect an increase in peak intensity at 550 and 630 nm along with decreasing intensity at 542 and 580 nm as time progresses. This pattern is displayed in **Figure 3-1B**, as expected.

Furthermore, normalized absorbance (A/A_0) data from electron transfer experiments plotted in **Figure 3-3** illustrate a much larger decline in A/A_0 than is observed in auto-oxidation experiments. As plotted in **Figure 3-2**, A/A_0 takes longer than 2 hours to drop below 0.8 by auto-oxidation in all tested samples. **Figure 3-3** shows all electron transfer samples falling below 0.8 A/A_0 within 20 minutes.

Figure 3-4 plots $\ln([MbO_2]/[MbO_2]_0)$ vs time and displays MbO_2 auto-oxidation kinetics with no FA and with equimolar quantities of OA, PA, and LA. The following first order rate constants (k) were estimated via linear regression from the slopes: without FA: k = 0.002 ± 1.44E-4 min^{-1} (R^2 = 0.9928), with OA: 0.0025 ± 5E-5 min^{-1} (R^2 = 0.9816), with PA: 0.0023 ± 5E-5 min^{-1} (R^2 = 0.991), with LA: 0.0021 ± 1E-4 min^{-1} (R^2 = 0.9927).

Figure 3-5 plots $1/[MbO_2]$ vs time for the MbO_2 electron transfer reaction to Cyt C^{3+} with and without FA and with equimolar quantities of OA, PA, and LA. The linear regression of the kinetics data yields the following second order rate constants (k): without FA: 0.5261 ± 0.046 mM^{-1} min^{-1} (R^2 = 0.9997), with OA: 0.5873 ± 0.0818 mM^{-1} min^{-1} (R^2 = 0.9967), with PA: 0.4373 ± 0.0234 mM^{-1} min^{-1} (R^2 = 0.9989), with LA: 0.3915 ± 0.01655 mM^{-1} min^{-1} (R^2 = 0.9982).

DISCUSSION

The present study set out to examine the impact of FA interaction on the redox properties of Mb, both by testing auto-oxidation and redox with Cyt C. The k values estimated in **Figure 3-4** and **Figure 3-5** suggest significant adjustment of both auto-oxidation and electron transfer rates, albeit not uniformly. Specifically, Mb auto-oxidation is significantly accelerated upon adding OA ($p = 0.03$), with $t_{1/2}$ decreasing from 346.6 min to 277.26 min. No such change in rate is observed when adding PA ($p = 0.12$) or LA ($p = 0.59$). By contrast, electron transfer to Cyt C is significantly slowed by the addition of LA ($p = 0.0287$), increasing reaction $t_{1/2}$ from 38.02 min to 51.09min. The addition of OA ($p = 0.55$) or PA ($p = 0.124$) does not induce a significant change in rate. Prior ^{1}H NMR experiments have measured large perturbations in Mb signal upon titration of LA, with much smaller signal shifts observed upon addition of PA (7). Together, these findings may suggest a significant difference in how PA and LA bind to Mb, pending future experiments.

CONCLUSION

An accumulating body of research raises provocative questions about myoglobin's function in the cell. It is an inefficient oxygen transporter at physiological pO_2 (9, 10), exhibits interesting, if largely unexplored, redox chemistry with cytochrome c (19), and perhaps the most significant change in MbKO mice appears to be an increased metabolic preference for carbohydrates over fatty acids (6). Grabbing hold of the puzzle presented by the fat averse MbKO mouse, the present study has attempted to explore some of the unanswered questions about a protein many believe has been thoroughly studied. Adding to recent experiments raising

the possibility of a robust role for myoglobin in fatty acid metabolism, the measurement of myoglobin redox modulation by fatty acid provides fodder for future research. Myoglobin's centrality as a model for the link between protein structure and function presents the rationale for further study, and the many questions remaining about myoglobin – fatty acid interactions provide a path forward.

Figure Captions

Figure 3-1

A) Reference spectra of 8 µM MbO_2, MetMb, Cyt C^{3+}, and Cyt C^{2+} at 35°C in 30 mM Tris/1 mM EDTA buffer pH 7.40 at 35°C. MbO_2 maxima appear at 542 and 580 nm; MetMb, 630 nm; Cyt C^{3+}, 530 nm; Cyt C^{2+}, 520 and 550 nm.

B) UV-Visible spectra at various timepoints for the electron transfer reaction between 0.05 mM MbO_2 and 0.05 mM Cyt C^{3+} in 30 mM Tris and 1 mM EDTA at pH 7.4 and 35°C. The MbO_2 peaks at 542 and 580 nm and the Cyt C^{3+} peak at 530 nm decrease while the Cyt C^{2+} peaks at 520 and 550 nm and the metMb peak at 630 nm increase. Spectra were acquired every 5 min over the 120 min time course.

Figure 3-2

Plot of normalized absorbance vs time for auto-oxidation of 0.05 mM MbO_2 in 30 mM Tris and 1 mM EDTA at pH 7.4 and 35°C, by itself and with equimolar quantities of OA, PA, and LA. The MbO_2 peak at 580nm was chosen for the large difference in extinction coefficient between the two Mb species. Spectra were acquired every 5 min over the 120 min time course.

Figure 3-3

Plot of normalized absorbance vs time for the electron transfer reaction between 0.05 mM MbO_2 and 0.05 mM Cyt C^{3+} in 30 mM Tris and 1 mM EDTA at pH 7.4 and 35°C. The experiment was repeated without FA and with equimolar quantities of OA, PA, and LA. The MbO_2 peak at

580nm was chosen for the large extinction coefficient of MbO_2 as compared to MetMb and the two Cyt C species. Spectra were acquired every 5 min over the 120 min time course.

Figure 3-4

Plot of ln $([Mb]/[Mb]_0)$ vs time for the auto-oxidation of 0.05 mM MbO_2 in 30 mM Tris and 1 mM EDTA at pH 7.4 and 35°C, by itself and with equimolar quantities of OA, PA, and LA. The following first order rate constants (k) were estimated via linear regression from the slopes: without FA: k = 0.002 ± 1.44E-4 min^{-1} (R^2 = 0.9928), with OA: 0.0025 ± 5E-5 min^{-1} (R^2 = 0.9816), with PA: 0.0023 ± 5E-5 min^{-1} (R^2 = 0.991), with LA: 0.0021 ± 1E-4 min^{-1} (R^2 = 0.9927).

Figure 3-5

Plot of $\frac{1}{[Mb]}$ vs time for the electron transfer reaction between 0.05 mM MbO_2 and 0.05 mM Cyt C^{3+} in 30 mM Tris and 1 mM EDTA at pH 7.4 and 35°C. The experiment was repeated without FA and with equimolar quantities of OA, PA, and LA. The following second order rate constants (k) were estimated via` linear regression from the slopes: without FA: 0.5261 ± 0.046 mM^{-1} min^{-1} (R^2 = 0.9997), with OA: 0.5873 ± 0.0818 mM^{-1} min^{-1} (R^2 = 0.9967), with PA: 0.4373 ± 0.0234 mM^{-1} min^{-1} (R^2 = 0.9989), with LA: 0.3915 ± 0.01655 mM^{-1} min^{-1} (R^2 = 0.9982).

References

1. **Antonini E, and Brunori M**. *Hemoglobin and Myoglobin in their Reactions with Ligands*. Amsterdam: North-Holland Publishing Company, 1971.
2. **Baron CP, and Andersen HJ**. Myoglobin-Induced Lipid Oxidation. A Review. *Journal of Agricultural and Food Chemistry* 50: 3887-3897, 2002.
3. **Chung Y, Huang S-J, Glabe A, and Jue T**. Implication of CO inactivation on myoglobin function. *American Journal of Physiology-Cell Physiology* 290: C1616-C1624, 2006.
4. **Garry DJ, Ordway GA, Lorenz JN, Radford NB, Chin ER, Grange RW, Bassel-Duby R, and Williams RS**. Mice without myoglobin. *Nature* 395: 905-908, 1998.
5. **Glabe a, Chung Y, Xu D, and Jue T**. Carbon monoxide inhibition of regulatory pathways in myocardium. *The American journal of physiology* 274: H2143-2151, 1998.
6. **Godecke A, Flogel U, Zanger K, Ding Z, Hirchenhain J, Decking UKM, and Schrader J**. Disruption of myoglobin in mice induces multiple compensatory mechanisms. *Proceedings of the National Academy of Sciences* 96: 10495-10500, 1999.
7. **Jue T, Shih L, and Chung Y**. Differential Interaction of Myoglobin with Select Fatty Acids of Carbon Chain Lengths C8 to C16. *Lipids* 52: 711-727, 2017.
8. **Jue T, Simond G, Wright TJ, Shih L, Chung Y, Sriram R, Kreutzer U, and Davis RW**. Effect of fatty acid interaction on myoglobin oxygen affinity and triglyceride metabolism. *Journal of Physiology and Biochemistry* 73: 359-370, 2016.
9. **Lin PC, Kreutzer U, and Jue T**. Anisotropy and temperature dependence of myoglobin translational diffusion in myocardium: Implication for oxygen transport and cellular architecture. *Biophysical Journal* 92: 2608-2620, 2007.
10. **Lin PC, Kreutzer U, and Jue T**. Myoglobin translational diffusion in rat myocardium and its implication on intracellular oxygen transport. *Journal of Physiology* 578: 595-603, 2007.
11. **Olivas E, de Waal DJA, and Wilkins RG**. Reduction of Metmyoglobin by Dithionite Ion *. 252: 4038-4042, 1977.
12. **Rodkey FL, and Ball EG**. Oxidation-reduction potentials of cytochrome c. *Fed Proc* 6: 286, 1947.
13. **Shih L, Chung Y, Sriram R, and Jue T**. Interaction of Myoglobin with Oleic Acid. *Chem Phys Lipids* 91: 165-171, 2015.
14. **Shih L, Chung Y, Sriram R, and Jue T**. Palmitate interaction with physiological states of myoglobin. *Biochimica et Biophysica Acta - General Subjects* 1840: 656-666, 2014.
15. **Sriram R, Kreutzer U, Shih L, and Jue T**. Interaction of fatty acid with myoglobin. *FEBS Letters* 582: 3643-3649, 2008.
16. **Taylor JF, and Morgan VE**. Oxidation-Reduction Potentials of the Metmyoglobin-Myoglobin System. *Journal of Biological Chemistry* 15-20, 1942.
17. **Wittenberg BA, and Wittenberg JB**. Transport of Oxygen in Muscle. *Annu Rev Physiol* 51: 857-878, 1989.
18. **Wittenberg JB**. Myoglobin-Facilitated Oxygen Diffusion: Role of Myoglobin in Oxygen Entry into Muscle. *Physiological reviews* 50: 559-636, 1970.
19. **Wu CS, Duffy P, and Brown WD**. Interaction of myoglobin and cytochrome C. *Journal of Biological Chemistry* 247: 1899-1903, 1972.

Figure 3-1

A

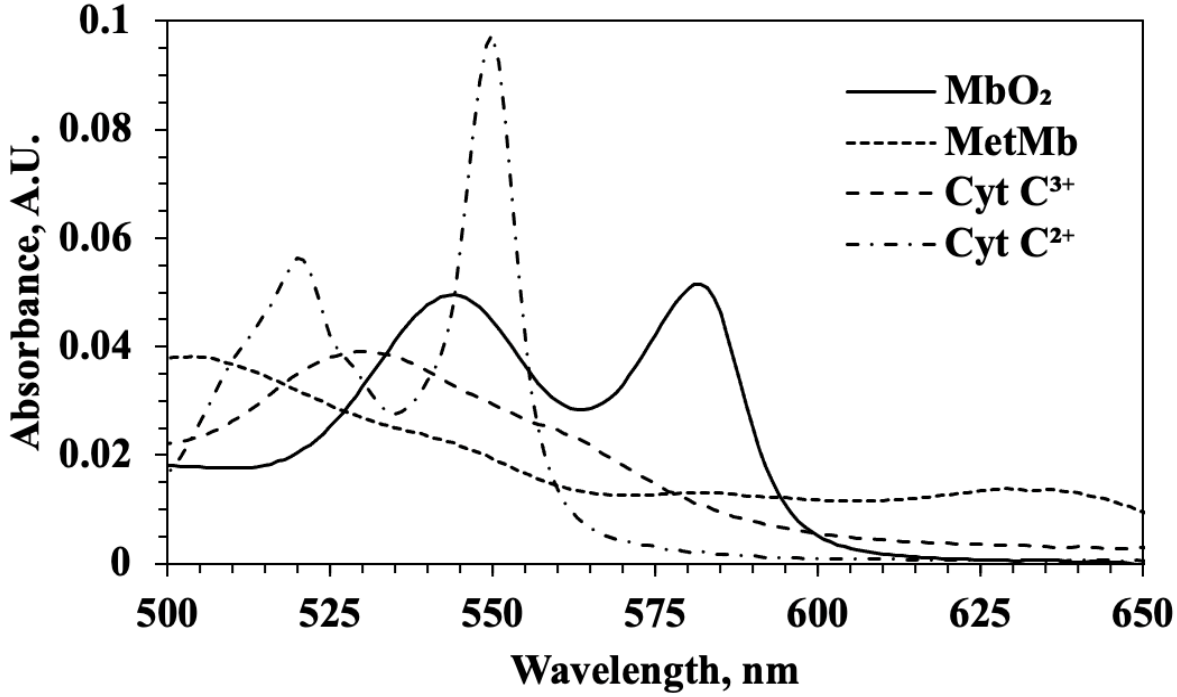
0.1
0.08
0.06
0.04
0.02
0
Absorbance, A.U.
500
525
550
575
600
625
650
Wavelength, nm
MbO₂
MetMb
Cyt C³⁺
Cyt C²⁺

B

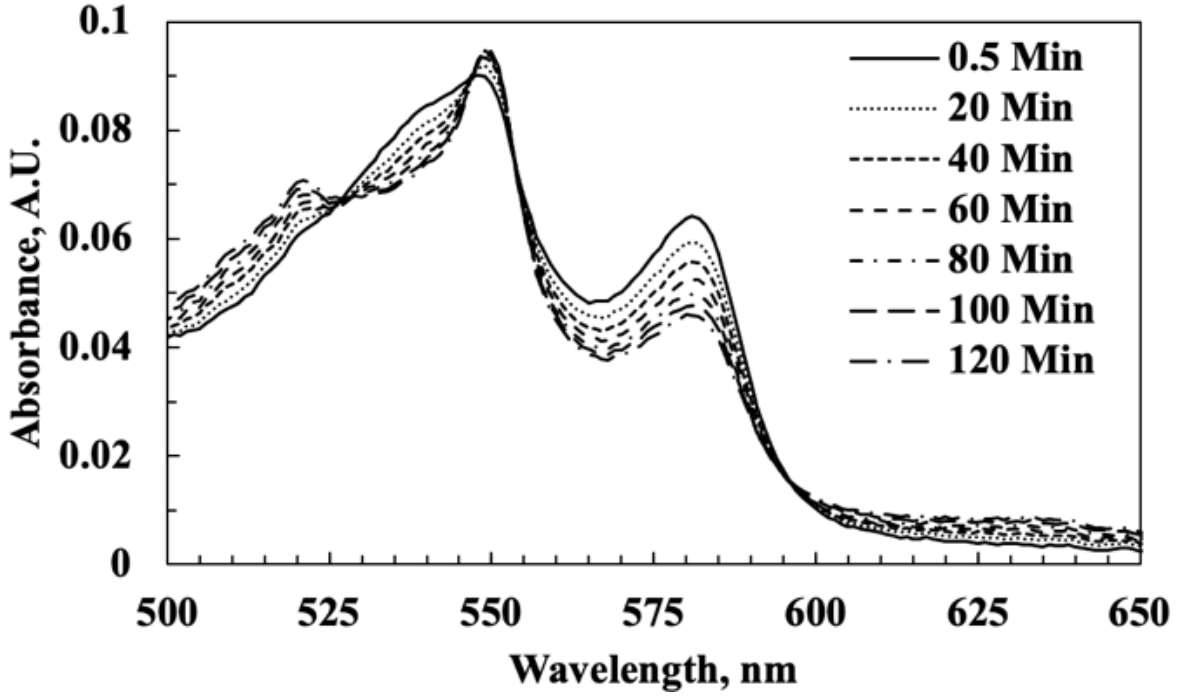
0.1
0.08
0.06
0.04
0.02
0
Absorbance, A.U.
500
525
550
575
600
625
650
Wavelength, nm
0.5 Min
20 Min
40 Min
60 Min
80 Min
100 Min
120 Min

Figure 3-2

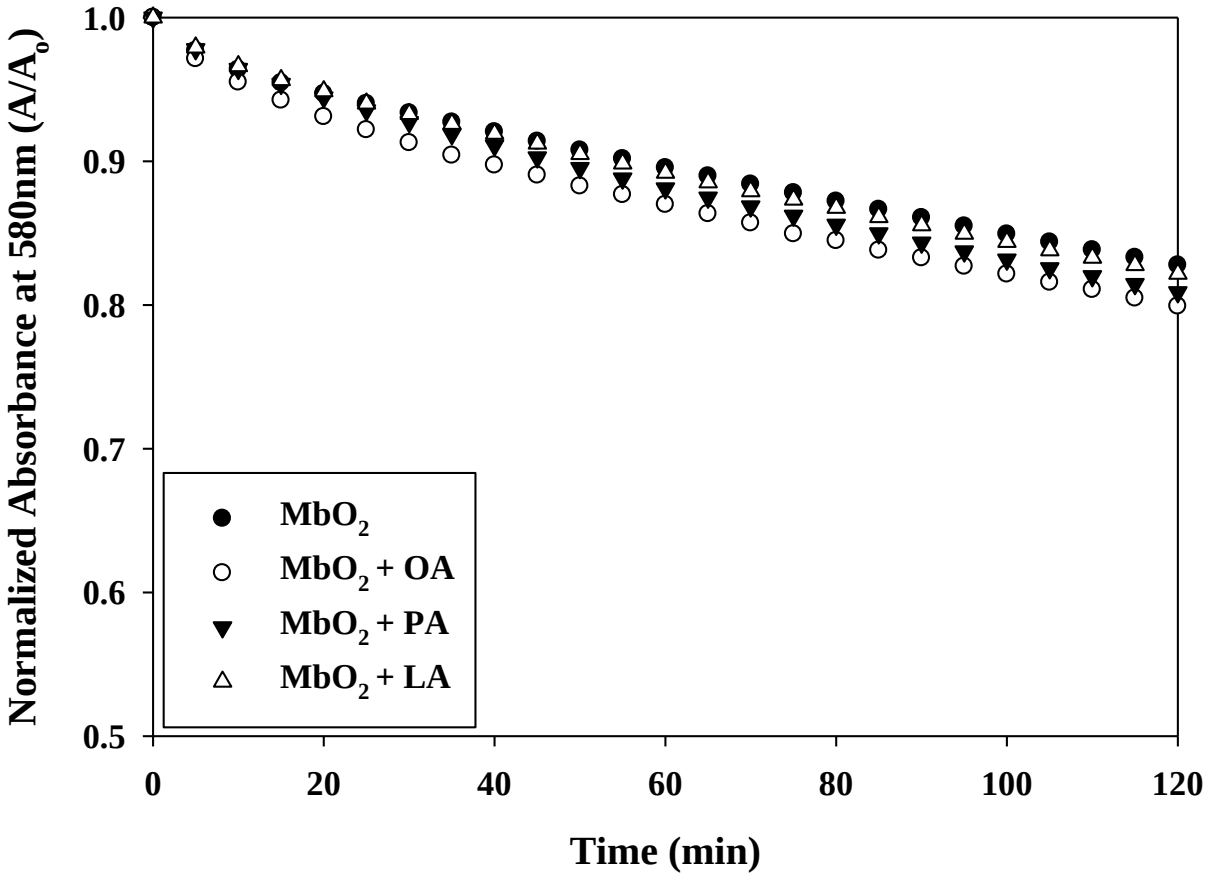
Normalized Absorbance at 580nm (A/A$_o$)
1.0
0.9
0.8
0.7
0.6
0.5
0
20
40
60
80
100
120
Time (min)
MbO$_2$
MbO$_2$ + OA
MbO$_2$ + PA
MbO$_2$ + LA

Figure 3-3

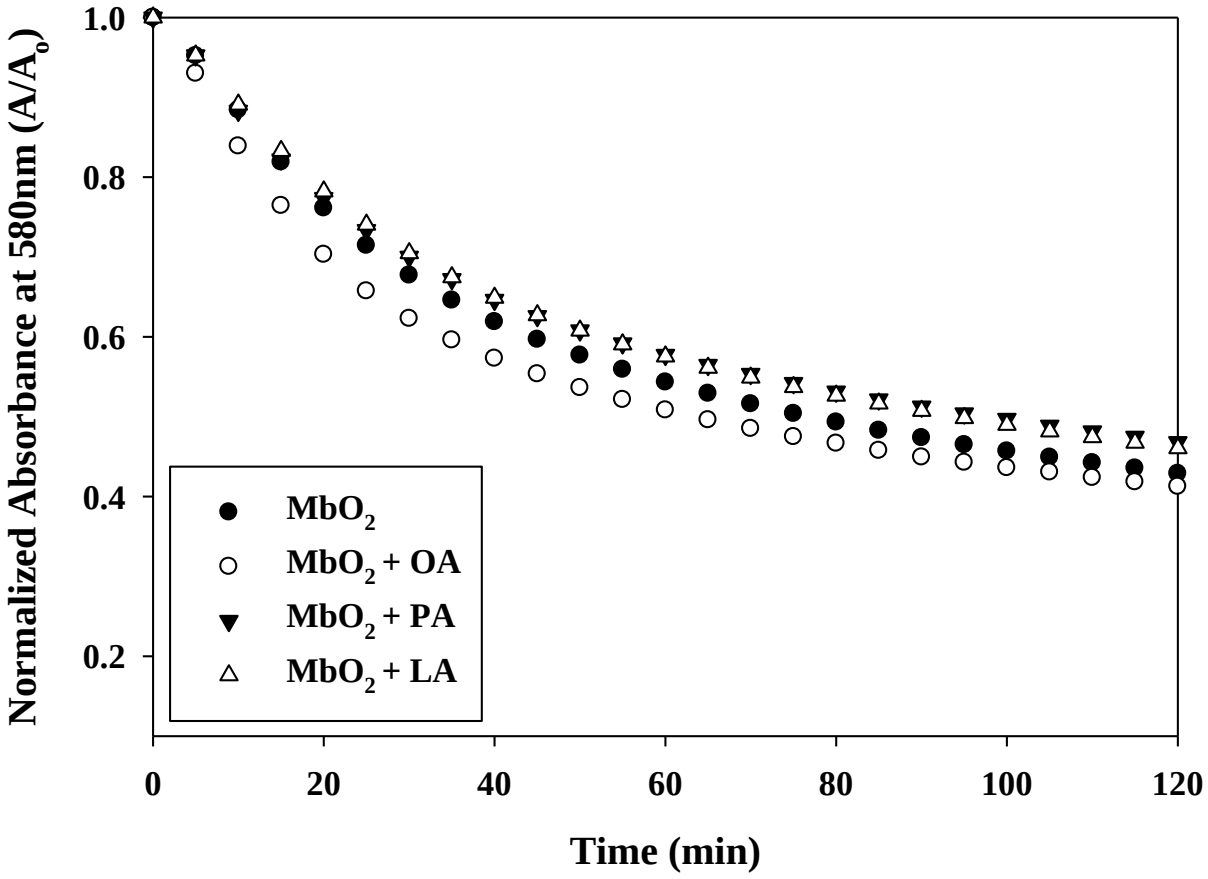
Normalized Absorbance at 580nm (A/A$_o$)
1.0
0.8
0.6
0.4
0.2
0
20
40
60
80
100
120
Time (min)
MbO$_2$
MbO$_2$ + OA
MbO$_2$ + PA
MbO$_2$ + LA

Figure 3-4

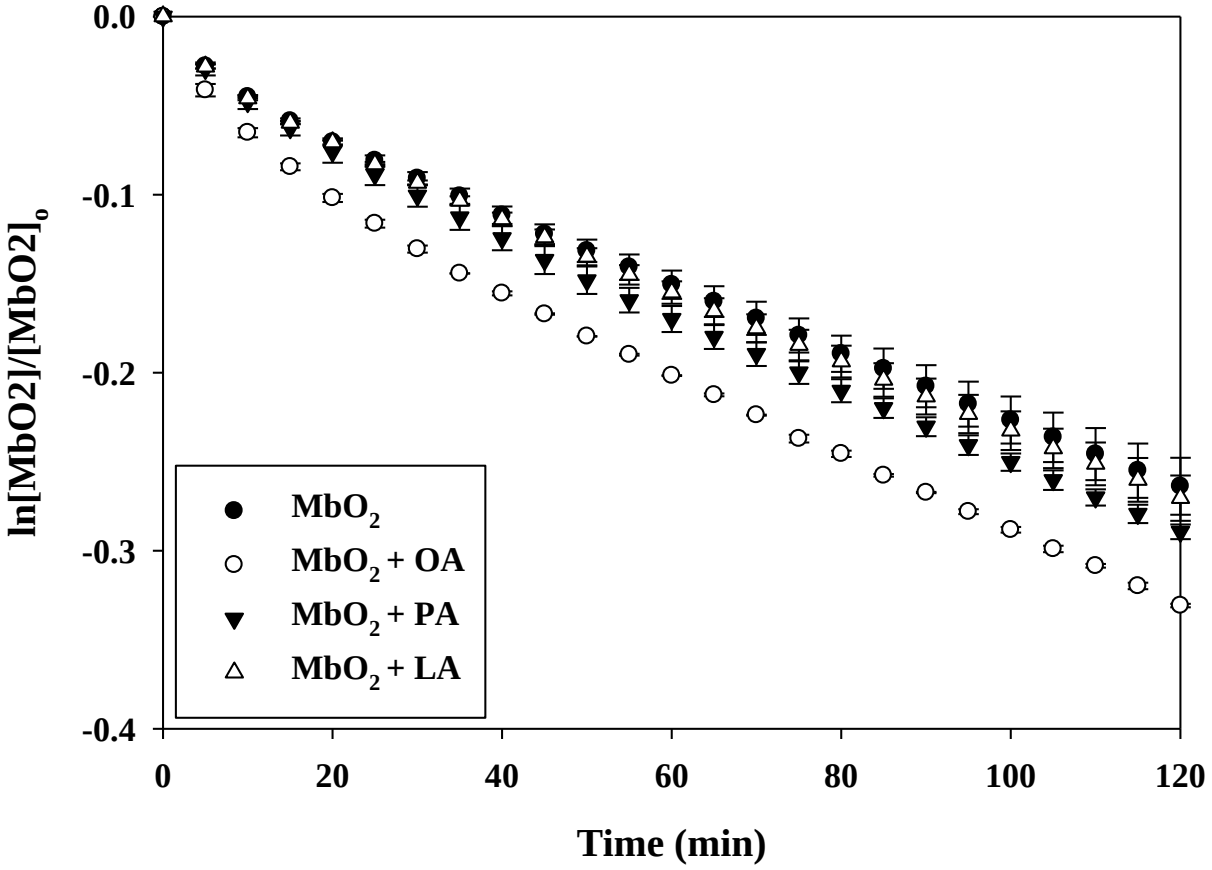
0.0
-0.1
-0.2
-0.3
-0.4
ln[MbO2]/[MbO2]o
0
20
40
60
80
100
120
Time (min)
MbO2
MbO2 + OA
MbO2 + PA
MbO2 + LA

Figure 3-5

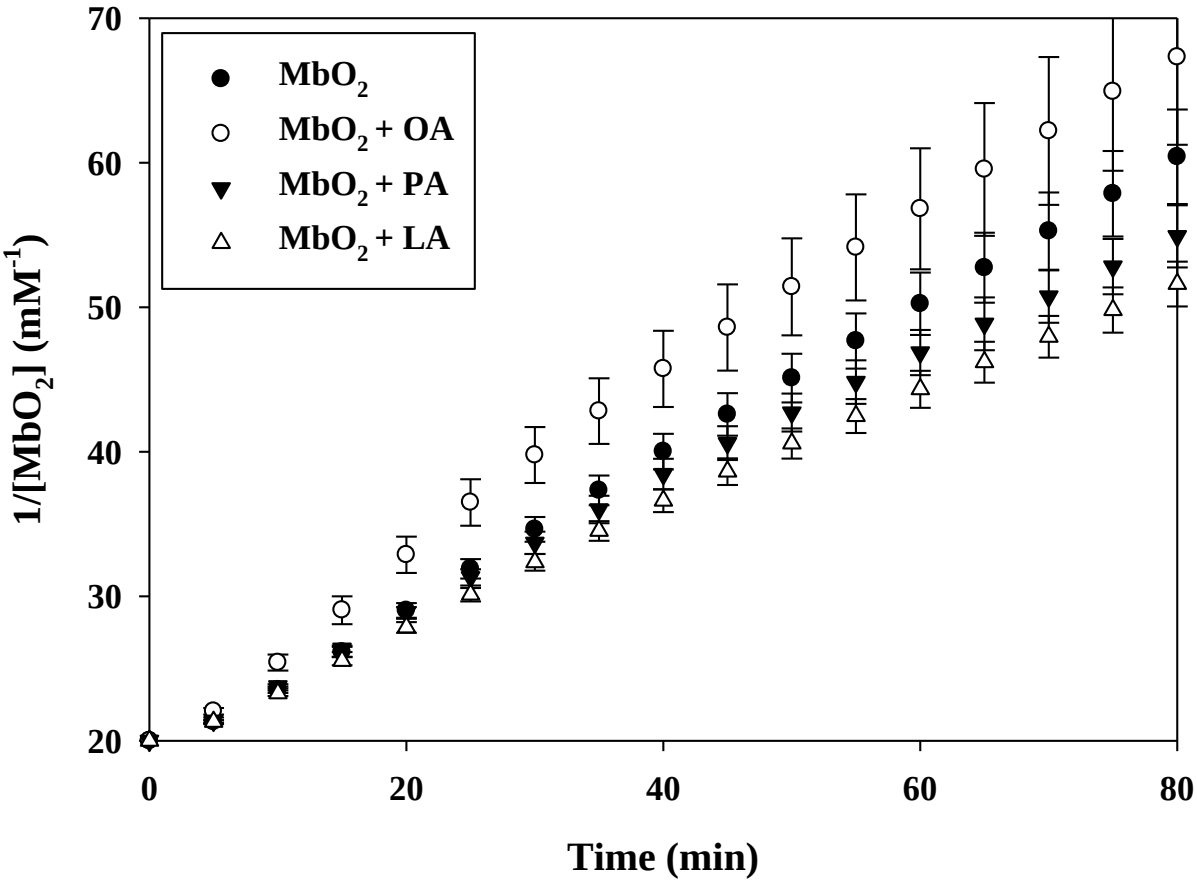
70
60
50
40
30
20
0
20
40
60
80
1/[MbO2] (mM-1)
Time (min)
MbO2
MbO2 + OA
MbO2 + PA
MbO2 + LA